**List of Contents**

## Acknowledgments

I would like to thank Prof. Michael Keusgen for providing me an interesting subject for my diploma thesis and for his support.

I would like to thank Mr. Doru Vornicescu, my German supervisor, who assisted and guided me throughout the whole project and helped me throughout my whole stay.

Also I thank all members of the working group in Marburg for all their support.

I want to thank Dr. Jarmila Jedelska for her support on my thesis and for making me feel at home there in Marburg.

At last I would like to thank my family for their support and for enabling me stay in Marburg.

Thank you all

# 1. Introduction

The primary mineral of the tooth enamel is hydroxyapatite and it gives rigidity for the tooth. All oral surfaces are covered with a pellicle system which composes of salivary components. This pellicle system represents the first barrier for oral microbial pathogens; or rather it modulates the adsorption of biofilm oral microbes. The identification of interacting mechanisms between oral micro flora, saliva and the pellicle system in oral cavity is an essential basis for understanding the formation of oral biofilms.

Surface Plasmon Resonance (SPR) is a well known method for testing thin layers and it is the sensitive surface analytical method for chemical and biochemical sensing. Sensors based on the resonance surface plasmon allow monitoring processes accompanied by a change in refractive index near the sensor surface in real time.

Sensors which were prepared in this work were used to monitor the absorption of the protein solution on the surface of the artificial tooth. Benefits of the sensor which was prepared by the electrophoresis could be time dependent monitoring of the reaction, for example determining the kinetic parameters.

This study was performed to evaluate the effects of two different saliva samples. The first one is native saliva while the second one is artificial saliva on the hydroxyapatite layer. Subsequently different solutions of the chlorhexidin gluconate pharmaceuticals were tested on the pellicle via Surface Plasmon Resonance.

## 2. Aim of the work

The aim of the diploma project was to develop an artificial tooth especially to find and optimize the method of coating gold chips with hydroxyapatite. As pellicle forming substrates pooled human and artificial saliva were used. To simulate the influence of therapeutic additives on the pellicle forming, a chlorhexidindigluconate preparate was selected. Two different solutions of mouth medication chlorhexidine were purchased from the pharmacy and measured by means of the SPR equipment. The first solution was Chlorhexamed 0.06 % ® with flour, while the second one was Chlorhexamed Fluid 0.1% ®.

# 3. Theoretical Part

## 3.1 Biosensors

A biosensor uses a biological system to measure a substance and differentiate this from other substances in a test sample. It is a measurement device that is composed of three components: a biological component (enzymes, nucleic acids, antibodies, bacteria, animal or vegetable tissues etc.) of appropriate specificity for the analyte (or the test material to be measured); a transducer to convert the recognition event into a suitable physical signal (electrical, optical etc.), and a detection and recording system, including analysis and processing, that is usually electrical or computer controlled (1). The principle and function of biosensors is schematically represented in Fig. 3.1.

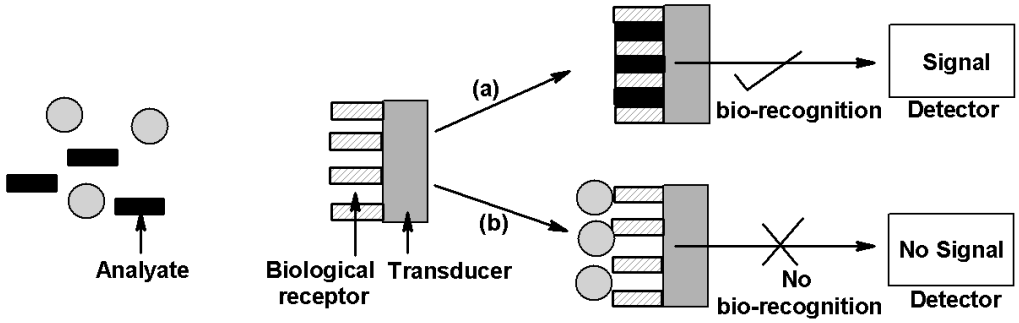


**Fig. 3.1:** Schematic representation of the principle and functioning of a biosensor showing the biological receptor, transducer and the detector.

(a) Bio-recognition due to binding of the analyte (black rectangle) to its specific biological receptor is converted by the transducer into a physical signal, which is received and recorded by the detector. (b) Substances (grey circles) not recognized by the biological receptor do not result in any detection signal.

## 3.1.1 Classification of Biosensors

### 3.1.1.1 Electrochemical Sensors

The basic principle of electrochemical sensors is that the electro active analyte species is oxidised or reduced on the working electrode surface, which is subjected to some predefined pattern of fixed or varying potential. The change in electrical parameters resulting from this redox reaction, as a function of the type or concentration of analyte, is measured (2). Three options are available, namely, amperometric, potentiometric and conductometric, each with their inherent advantages and disadvantages (3). Electrochemical sensors have found wide application in food and medical applications (2). In electrochemical sensing, at present, the usual electrode configuration involves a three electrode arrangement: The working electrode, where the electron transfer reaction takes place, the reference electrode, which maintains a stable potential with respect to the working electrode and the auxiliary electrode, made of inert conducting material like Pt, graphite etc.; with some supporting electrolyte for the electrode to eliminate electro migration effects, decrease solution resistivity and maintain the ionic strength constant (4). Choosing the working electrode material is fundamental to the success of the assay. Development of microelectrodes (<2mm dimension) has opened the horizon of in vivo and in vitro applicability of electrochemical sensor systems requiring only micro liter volumes of analyte and reagent (3).Screen-printed electrodes (5), which involves deposition of electrode material, mainly carbon and noble metals, on inert PVC or ceramic supports has been a breakthrough in the advancement of electrochemical biosensors. The use of materials like carbon nanotubes (CNT) and nanoparticles are being explored to enhance the functionality, sensitivity and applicability of electrochemical sensors (2).

#### 3.1.1.1.1 Amperometric Sensors

Amperometric biosensors mostly use reduction-oxidation (redox) enzyme systems. The redox enzyme is immobilized on the surface of the electrode. The electrode is held at a fixed potential, adjusted so that electrons arising from an oxidised substrate are transferred to the electrode (or vice versa for a reduction reaction), and this regenerates the active form of a cofactor for another redox cycle. The enzyme used determines the specificity of the reaction. As the rate of enzymatic reaction at a fixed temperature and pH is directly proportional to the substrate concentration, the current produced at the electrode is proportional to the rate of modification of the substrate by the enzyme. The most well-known amperometric sensor, which is also considered to have pioneered the biosensor revolution, is the amperometric sensor detecting glucose level in blood developed by Clark and Lyons. This biosensor was used in continuous monitoring of glucose in cardiovascular surgery. Since the first glucose enzyme electrode based biosensor a lot of development (such as use of artificial mediators) has taken place in the area of glucose biosensors, though the underlying principle is still amperometric detection (6).

#### 3.1.1.1.2 Potentiometric Sensors

According to the definition provided by IUPAC, potentiometric measurements involve the determination of the potential difference between either an indicator or a reference electrode or two reference electrodes separated by a permselective membrane, where there is no significant current flowing between them (7). The transducer may be an ion-selective electrode (ISE), which is based on thin films or selective membranes as recognition elements. The most common potentiometric devices are pH electrodes; several other ion- (F-, I-, CN-, Na+, K+, Ca2+, NH4+) or gas- (CO2, NH3) selective electrodes are available. The first potentiometric biosensor demonstrated was for the detection of urea (8). The enzyme urease was immobilized in a

layer of acrylamide polymer on the surface of a cationic electrode sensitive to ammonium ion. The substrate urea diffuses to the enzyme electrode and reacts with the immobilized enzyme to produce ammonium ion at the surface of the glass electrode. A thin film of cellophane was placed around the enzyme gel layer to prevent leaching of urease into the surrounding solution. Several potentiometric sensors use a transducer scheme based on potentiometric monitoring of local pH changes. An enzymatic pathway, which leads to change in hydrogen ion activity, can be applicable for this task. This principle has been used for the development of a potentiometric-penicillin-sensitive biosensor. The enzyme penicillase is used as the immobilized bio recognition element (9). Two other categories of potientiometric sensors use coated-wire electrodes (CWES) and field effect transistors (FET) as transducers (3).

#### 3.1.1.1.3 Conductometric Sensors

The principle of conductometric measurements is based on the detection of solution conductivity variations. Most of these devices are based on the fact that a large number of enzymatic reactions involve the production or consumption of charged species (9). Many enzyme reactions, such as that of urease, and activities of many biological membrane receptors may be monitored by ion conductometric devices (10). As the sensitivity of the measurement is hindered by the parallel conductance of the sample solution, usually a differential measurement is performed between a sensor with enzyme and an identical one without enzyme. Such a device has also been used in monitoring of heavy metal ions and pesticides in water samples (11). The bio recognition element used in this case was the micro algae *Chlorella vulgaris.*

#### 3.1.1.2 Nanomechanical Sensors

##### 3.1.1.2.1 Piezoelectric Mass Sensors

Mass detection sensors are among the most widely used micro analytical sensors. These methods rely in general on measuring the changes in vibrational resonant frequency of piezoelectric quartz oscillators that result from changes in mass on the oscillator's surface.

The most common form of such sensors is the quartz crystal microbalance (QCM) and the surface acoustic wave (SAW) device. The QCM device consists of a quartz crystal disk driven by electrodes on either face. The mass of analytes that bind to the sensor is measured as a change in the crystal's resonant frequency. This type of sensor is also known as a thickness-shear mode (TSM) device.

In the SAW sensor an acoustic wave is created by applying an alternate voltage to a metallised, inter-digitated electrode plated onto one end of a thin piezoelectric planar substrate of the device.

##### 3.1.1.2.2 Microcantilever Sensors

The principle of the cantilever biosensor is based on mechanical stresses produced in a sensor upon molecular binding. This stress bends the sensor mechanically and can easily be detected.

#### 3.1.1.3 Optical Sensors

Optical biosensors are a powerful detection and analysis tool that has vast applications in biomedical research, healthcare, pharmaceuticals, environmental monitoring and fight against biological threats (12). The main advantage of optical biosensors over electrochemical biosensors is that they are resistant to electromagnetic interference, capable of performing remote sensing, and can provide multiplexed detection within a single device. Generally, there are two broad detection protocols that can be implemented in optical bio sensing: labeled (e.g., fluorescence-based detection) and label-free detection.

#### 3.1.1.3.1 Optical Biosensors Using Labels

The most commonly used format of labeled optical biosensor uses fluorescence-based detection. In fluorescence-based detection, either target molecules or bio recognition molecules are labelled with fluorescent tags, such as dyes; the intensity of the fluorescence indicates the presence of the target molecules and the interaction strength between target and bio recognition molecules. While fluorescence-based detection is extremely sensitive, with the detection limit down to a single molecule (13) it suffers from laborious labeling processes that may also interfere with the function of a bio-molecule. Fluorescence based biosensors have been used in conjunction with Fiber-optics to create what are called optrode-based fibre optic biosensors (Bio-optrode) and evanescent wave Fiber optic biosensors.

Bio-optrodes are analytical devices incorporating optical fibers and biological recognition molecules. Optical fibers are small and flexible "wires" made out of glass or plastic that can transmit light signals with minimal loss over long distances. The light signals are generated by a sensing layer, which is usually composed of bio-recognition molecules and dyes, coupled to the fiber end. Light is transmitted through the optical fibers to the sensing layer, where different optical phenomena such as absorption or luminescence are used to measure the interactions between the analyte and the sensing layer. Bio-optrodes can be used for remote analytical applications including clinical, environmental, and industrial process monitoring (14).

Evanescent wave fiber optic biosensors differ from the optrodes with respect to the nature of the light used. In case of optrodes the light shining out of the end of the optic fiber is used to generate a signal either at the distal face of the fiber or in the medium near the fiber´s end. On the other hand, evanescent wave sensors rely on the electromagnetic component of the reflected light at the surface of the fiber core to excite only the signal events localized at that surface. Thus, in case of the evanescent fiber optic sensors the penetration depth of the light into the surrounding medium is much more restricted, than for optrodes, while the surface area interrogated is much

larger in comparison to optrodes of equal diameter. The result is that evanescent wave biosensors require immobilization of the biological recognition molecules onto the longitudinal surface of the optical fiber core (14).

Recently, the use of quantum dots as labeling agent has been used in the development of Fiber optic based biosensors (15). The quantum dots are semiconductor nanocrystals. Quantum dots have a number of unique properties that can be used in development of fluorescence and fluorescence resonance energy transfer (FRET) based biosensors (16).

#### 3.1.1.3.2 Label-free Optical Biosensors

The most commonly used optic biosensors fall into two broad categories based on the technology platform used. These are the evanescent wave biosensors and the interferometer-based biosensor. The different label free optical biosensors has been recently been reviewed by Fan et al. (2008). The most widely used evanescent wave optical biosensor is the Surface Plasmon Resonance biosensor.

#### Evanescent Wave Biosensors

The operation of these biosensors is based on the optical properties of thin metal films with high refractive index deposited on the surface of a glass prism. Light coming from the glass is totally internally reflected from the metal surface, and at a certain angle of incidence the excitation of resonance in the film produces intensity and phase changes in the reflected beam. An evanescent field is also generated which travels in a direction perpendicular to the surface. The detection of bio-molecular interaction is based on the fact that the resonance characteristic is very sensitive to changes of the refractive index in the evanescent field. The detailed description of the physics behind this phenomenon has been reviewed by Cush et al. (1993) and Raether (1997). Two types of optical biosensors based on this principle are Surface Plasmon Resonance (SPR) biosensor and the resonant mirror (RM) optical

biosensor. As both of these biosensors are based on monitoring changes in refractive index occurring with each bio-molecular interaction, no labeling of the analyte is required.

Surface Plasmon Resonance (SPR) biosensor was first demonstrated for biosensing by Liedberg et al. (1983). SPR sensors consist of a thin metallic layer (typically Au or Ag) of about 50 nm deposited directly onto a glass prism. The measurement principle is based on excitation of surface plasmons at the boundary between the metal film and the sensing layer. As a result, incident light is adsorbed, resulting in a decrease in the intensity of the reflected light. The angle of incidence of the exciting light is extremely sensitive to the refractive index occurring in the sensing film at the metal-film boundary. The fundamentals of SPR will be discussed in detail in section 3.1.2.1.

RM instruments are based on a waveguide structure (RM) (17), where the evanescent field results from the propagation of light along the waveguide. This waveguide is made from a metal oxide. Refractive index changes occurring due to bio-molecular interactions on the sensing layer, at the surface of the waveguide, alter the conditions under which the light couples in and travels along the guide. Monitoring these changes with time forms the basis of the measurement (18). Unlike SPR devices, the system is looking for a peak of intensity, not a decrease.

## 3.1.2 Surface Plasmon Resonance (SPR)

### 3.1.2.1 Fundamentals of SPR

Surface Plasmon Resonance (SPR) biosensors belong to the category of evanescent wave biosensors. When a light beam passes from a material having a relatively high refractive index (e.g., a glass prism) into a material having a lower refractive index (e.g., water), the light is bent towards the plane of interface. Total internal reflection occurs when the angle, at which the light strikes the interface, is greater than the critical angle. The critical angle is defined as the angle of incidence, which provides an angle of refraction of 90-degrees. SPR is observed under conditions of attenuated total internal reflection (ATR), when the surface of the prism coated with so-called “free electron metals” like gold is placed in contact with a dielectric material (buffer with sample). Surface Plasmon waves (SPW) are present on the gold surface due to the free-oscillating electrons. The basic setup of exciting SPW consists of coupling a prism coated with a thin metal in contact with a dielectric (Fig. 3.2). The excitation of the SPW at the interface of non-magnetic metals such as gold and a dielectric is possible only using the transverse magnetic mode (TM) of plane-polarised light.

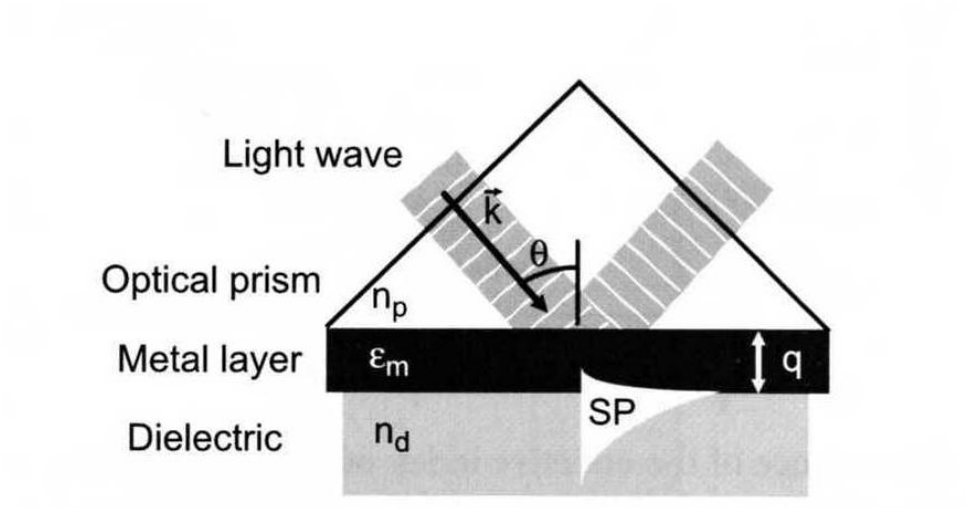


**Fig. 3.2:** Excitation of surface plasmons in the Kretschmann geometry of the attenuated total reflection (ATR) method.

When a light wave propagating in the prism is made incident on the metal film a part of the light is reflected back into the prism and a part propagates in the metal in the form of an inhomogeneous electromagnetic wave. This inhomogeneous wave decays exponentially in the direction perpendicular to the prism-metal interface and is therefore referred to as the evanescent wave. If the metal film is sufficiently thin (less than 100 nm), the evanescent wave penetrates through the metal film and couples with the surface plasmon at the outer boundary of the metal film.

At a particular angle of incidence, the propagation constant of the incident light matches with the propagation constant of the SPW, resulting in SPR. This angle, at which there is a minimum in the intensity of reflected light, is called the SPR angle. The propagation constant is defined as the product of the effective refractive index ($n_{eff}$) times the vacuum wave number and is represented by the equation:

$$\beta = n_{eff}\, 2\pi/\lambda \qquad (3.1)$$

Where $n_{eff}$ is the effective refractive index and has the analogous meaning for light propagation in a waveguide.

The propagation constant of the surface plasmon, propagating along the metal film $\beta^{SP}$ is influenced by the presence of the dielectric on the opposite side of the metal film and can be expressed as

$$\beta^{SP} = \beta^{SP0} + \lambda\beta \qquad (3.2)$$

$\beta^{SP}$ is the propagation constant of the surface plasmon wave and is defined by the equation:

$$\beta^{SP} = (2\pi/\lambda) n_p \sin\theta \qquad (3.3)$$

$n_p$ = refractive index of the prism

$\theta$ = incident angle of the TM polarised light

$\beta^{SP}$= propagation constant of the surface plasmon wave in the absence of the prism and is defined by the equation:

$$\beta^{SP_o} = \frac{2\pi}{\lambda}\sqrt{\frac{\varepsilon_d \times \varepsilon_m}{\varepsilon_d + \varepsilon_m}} \tag{3.4}$$

$\varepsilon_d$ = permittivity of the dielectric

$\varepsilon_m$ = permittivity of the metal

$\Delta\beta$= term accounting for the finite thickness of the metal film and the presence of the prism

The propagation constant of the evanescent field is defined as the real part of the $\beta^{SP}$ and is represented by the equation:

$$\beta^{EW} = \mathrm{Re}\left(\frac{2\pi}{\lambda}\sqrt{\frac{\varepsilon_d \times \varepsilon_m}{\varepsilon_d + \varepsilon_m}} + \Delta\beta\right) \tag{3.5}$$

For Surface Plasmon Resonance to occur the propagation constant of the surface plasmon ($\beta^{SP}$) should be equal to the propagation constant of the evanescent field.
($\beta^{EW}$).

Therefore from equations 1.3 and 1.5 :

$$\beta^{SP} = \frac{2\pi}{\lambda} n_p \sin\theta = \beta^{EW} = \mathrm{Re}\left(\frac{2\pi}{\lambda}\sqrt{\frac{\varepsilon_d \times \varepsilon_m}{\varepsilon_d + \varepsilon_m}} + \Delta\beta\right) \tag{3.6}$$

In terms of the effective refractive index, this coupling condition (1.6) can be written as follows:

$$n_p \sin\theta = n_{ef}^{EW} = n_{ef}^{SP} = \mathrm{Re}\left(\sqrt{\frac{\varepsilon_d \times \varepsilon_m}{\varepsilon_d + \varepsilon_m}} + \Delta n_{ef}^{SP}\right) \quad (3.7)$$

Where *EW ef n* is the effective refractive index of the evanescent wave
*SP ef n* is the effective refractive index of the surface plasmon, defined in equation (3.1)

The coupling condition is summarized in equation (3.3). According to this equation it is clear that for each wavelength and the corresponding effective refractive index, the matching condition is satisfied for a single angle ($\theta$) of incidence, the SPR angle. This is illustrated in Fig. 3.3.

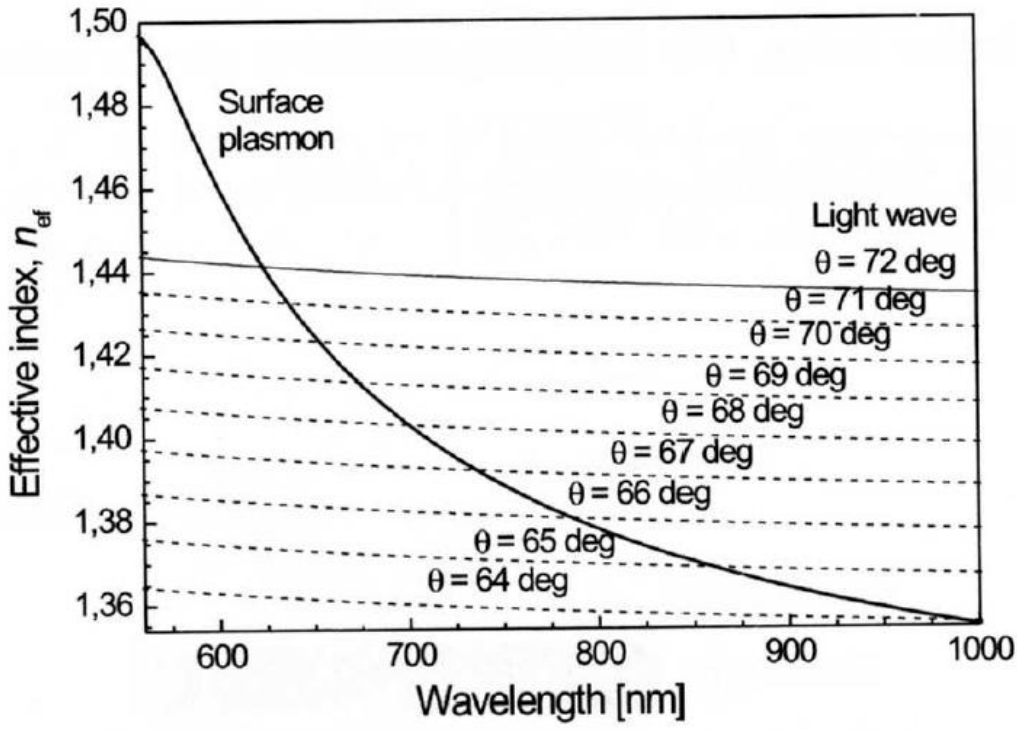


**Fig. 3.3:** Representative plot explaining the spectral dependence of the effective refractive index of a surface plasmon wave on the interface of gold-water, produced by a plane light wave incident on the gold film of an optical prism (BK 7 glass) at nine different angles of incidence.

This angle increases with decreasing wavelength. The SPR condition is also explained with respect to the effective refractive index as shown in equation (3.7). Two main configurations are used in the ATR method, namely the Kretschmann geometry and the Otto geometry. In the Kretschmann geometry of the ATR method, a high refractive index prism with refractive index $n_p$ is interfaced with a metal-dielectric waveguide consisting of a thin metal film with permittivity $\varepsilon_m$ and thickness q, and a semi-infinite dielectric with a refractive index $n_d$ ($n_d < n_p$) (Fig. 3.2).

In the Otto geometry, a high refractive index prism with refractive index $n_p$ is interfaced with a dielectric-metal waveguide consisting of a thin dielectric film with refractive index $n_d$ ($n_d < n_p$) and thickness q, and a semi-infinite metal with permittivity $\varepsilon_m$ (Fig. 3.4). Of the two geometries presented here, the Kretschmann configuration is most commonly used, probably due to the ease of construction. In case of this work the Plasmonic® SPR device used works on the Kretschmann configuration. The details of the device are presented in section.

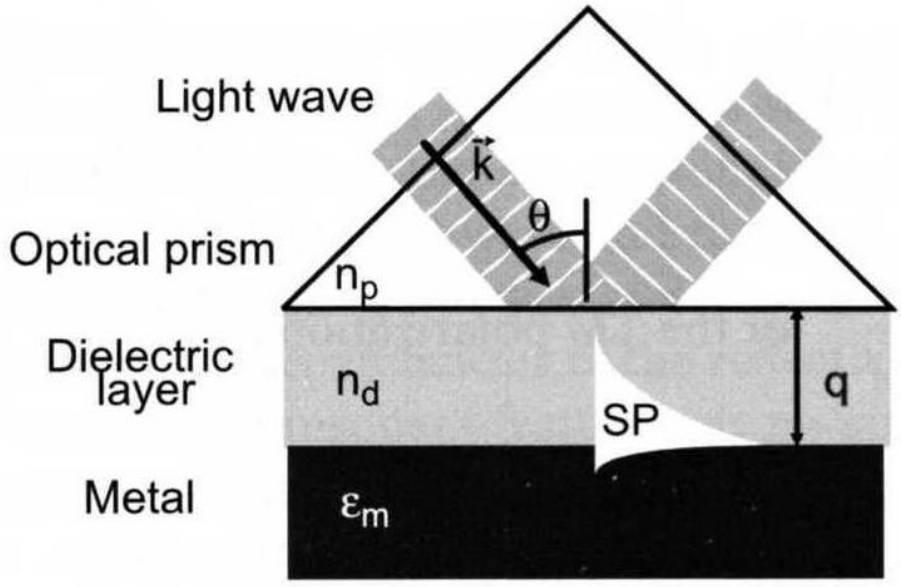


**Fig. 3.4:** Excitation of surface plasmons in the Otto geometry of the attenuated total reflection (ATR) method.

As mentioned, the evanescent wave produced during SPR is an exponentially decaying wave and has a penetration depth of about 100-200 nm into the dielectric (19). It is important to note that in case of SPR, when bio-molecular interactions occur on the gold surface (within the range of the penetration depth of the evanescent field) there is a change in refractive index of the dielectric Hample medium. This change in refractive index causes a change in the propagation constant of the SPW. Consequently, the angle at which SPR occurs also changes. This change is recorded as a shift in the SPR angle with time, resulting in SPR sensor grams. For each SPR angle there is a minimum in the intensity of reflected light. This change in angle, corresponding to the minimum in reflected light, is directly proportional to the loading of bio-molecules on the gold surface of the SPR prism (20).

#### 3.1.2.2 Detection Formats in SPR

In SPR assays the detection format is chosen based on the size of target analyte molecules, binding characteristics of available bio-molecular recognition element, range of concentrations of analyte to be measured, and sample matrix (21). The following four formats are commonly used in SPR based assays:

**(a) Direct Detection**:

In the direct detection mode (Fig. 3.5a), the bio recognition element (e.g., antibody) is immobilized on the SPR sensor surface. Analyte in solution binds to the antibody, producing a refractive index change, which is detected by the SPR sensor. Direct detection is usually preferred in applications, where direct binding of analyte of interest produces a sufficient change in the refractive index.

**(b) Sandwich Detection:**

The specificity and limit of detection of the direct assay can be improved by using the sandwich detection format (Fig. 3.5 b), in which the sensor surface with captured analyte is incubated with a second detection antibody. Smaller analytes having molecular weight less than 5000 Daltons often do not

generate a sufficient change in the refractive index (22) and are therefore measured using either the competitive or the inhibition detection format.

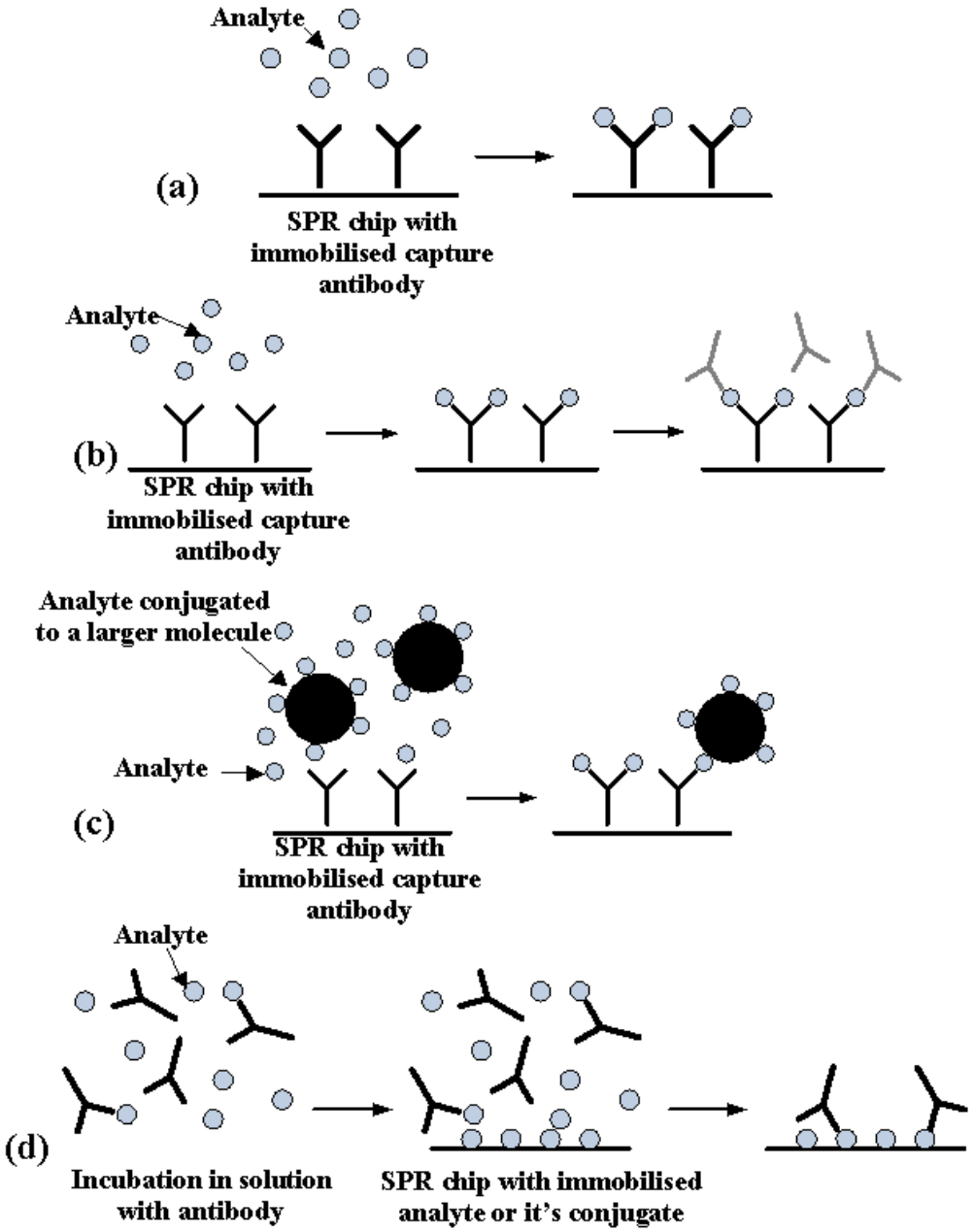


**Fig. 3.5:** Different detection formats used in SPR assays (a) direct detection (b) sandwich detection (c) competitive detection (d) inhibition detection.

**(c) Competitive Detection:**

In the competitive detection format the sensing surface is coated with an antipody interacting with the analyte; when an analyte conjugated to a large molecule is added to the sample, the analyte and its conjugated analogue compete for a limited number, of binding sites on the surface. The binding response is inversely proportional to the analyte concentration (Fig. 3.5 c).

**(d) Inhibition Detection:**

In the inhibition detection format (Fig. 3.5 d) a fixed concentration of an antipody with affinity to analyte is mixed with a sample containing an unknown concentration of analyte. Then, the mixture is passed over a sensor surface to which the analyte or its analogue is immobilized. Antibodies, which do not bind to the analyte in solution, are measured as they bind to the analyte molecules immobilized on the sensor surface. The binding response is inversely proportional to the concentration of analyte.

### 3.1.2.3 Biorecognition Elements in Surface Plasmon Resonance

In SPR biosensors, one of the interacting molecules is immobilized on the solid surface of the SPR sensor and the other is contained in a liquid sample. Which of the molecules is immobilized depends on the used detection format (section 3.1.2.2). In case of the direct, sandwich and competitive detection formats the molecule that needs to be immobilized is a bio-recognition element. In the inhibition detection format, the immobilized molecules are the target molecules or their derivatives. The choice of appropriate bio-recognition elements and immobilization methods is of critical importance with direct impact on key performance characteristics of the sensor such as sensitivity, specificity, and limit of detection of the assay.

**Bio-recognition Elements**

Various kinds of bio-recognition elements have been employed in affinity SPR biosensors. Antibodies remain by far the most frequently used biorecognition elements. They offer high affinity and specificity against target

analyte. Moreover, antibodies against numerous target molecules are now commercially available. The structure and properties of antibodies is discussed in section recently, single-chain antibody fragments (scFvs) have been used as bio-recognition elements (23). Biotinylated scFv fragments expressed in yeast can be spotted on streptavidin-coated sensor surfaces directly from cell supernatant without the need for purification (24). Another type of bio-recognition element that has been employed in SPR sensors are peptides. In comparison with antibodies, peptides, in general, are inexpensive, more stable, and easier to manipulate. However, peptides sometimes lack high affinity and specificity against the target. In SPR biosensors, peptides have been applied mainly for the detection of antibodies, for example, antibodies against hepatitis, herpes simplex virus type 1 and type 2, (25) and Epstein-Barr virus (26), and also for the detection of heavy metals (27). Recently, aptamers emerged as another promising type of bio-molecular recognition element for SPR biosensors (28). DNA or RNA aptamers are single-stranded oligonucleotide sequences, which can be produced to bind to various molecular targets such as small molecules, proteins, nucleic acids, and even cells, tissues and organisms (29).

**Immobilisation of Bio-recognition Elements**

In SPR biosensors, one of the interacting molecules (mostly the bio-recognition element) is immobilized on the sensor surface. The surface chemistry has to be designed in such a way that it enables immobilization of a sufficient number of bio-recognition elements on the sensing surface while minimizing the non-specific binding to the surface. In addition, bio-recognition elements need to be immobilized on the sensor surface without affecting their biological activity. In principle, the molecules can be immobilized either on the surface or in a three-dimensional matrix. Although immobilization on surfaces is more straightforward to perform, the number of accessible bio-recognition elements is limited by a number of factors such as orientation on the surface and steric hindrance. Immobilization in a three dimensional matrix

is an approach to obtain more binding sites than immobilization on the surface (30). The most widely used three-dimensional matrix for immobilisation of molecules in a structured environment is the carboxymethylated dextran matrix (31). For two-dimensional surface immobilisation of bio-recognition elements on the sensing gold surface, self-assembled monolayers (SAMs) of alkanethiols or disulfides have been widely used (32). To provide a desired surface concentration of bio-molecular recognition elements and a non-fouling background, mixed SAMs of long-chained alkanethiols terminated with a functional group for further attachment of bio-molecular recognition elements and oligo(ethylene glycol) terminated shorter-chained alkanethiols for a non-fouling background have been developed (33). The main approaches to immobilization of molecules to the surface of SPR sensors are based on physical adsorption involving hydrophobic and electrostatic interactions (34), covalent coupling (31). Another approach is based on attachment of tagged molecules by a site-specific non-covalent interaction between the tag and an immobilized capture molecule via biotin-avidin (35) or histidine-chelated metal ion (36) interaction or DNA hybridisation (37). Recently, Rusmini (38) has provided a general overview of different immobilization strategies. However, biosensors based on enzymes or antibodies often suffer from poor immobilization of the biological component. This leads to partial loss of function, sensitivity or lifetime of the sensor. Most immobilization methods are based on unspecific cross-linking of functional groups of the protein, mostly amine or carboxyl functions (22). As all these methods are not site-directed they often result in a partial or complete loss of the function of the bio-molecule. In case of antibodies, the most common immobilization procedures are based on capturing amino functions. This is rather crucial for the binding of antibodies because terminal amino functions are placed in the recognition area. This usually results in functional loss of antibodies. In addition, amine and carboxyl groups are known to be well distributed on the surface of the antibody. Thus, immobilization procedures using these functional groups will

randomly orient the antibody making the binding site unavailable to the antigen (39). In recent years, there has been a shift in focus to develop biosensors for the rapid detection of pathogens. SPR has been successfully used for the rapid detection of different pathogens (40).

## 3.3 Anatomy and Physiology of Human Teeth

### 3.3.1 The Teeth (*dentes)*

The teeth are hard conical structures se in the dental alveoli (tooth sockets) of the upper and lower jaws and are used in mastication (chewing) and assisting in articulation. Children have 20 deciduous (primary) teeth. The first tooth usually erupts at 6-8 months of age and the last tooth by 20-24 months of age.

A tooth has a crown (*corona*), neck (*cervix*), and root. The crown projects from the gingiva. The neck is between the crown and the root. The root is fixed in the tooth socket by the *periodontium*; the number of roots varies. Most of the tooth is composed of dentin, which is covered by enamel over the crown and cement over the root. The pulp cavity contains connective tissue, blood vessels, and nerves. The root canal (*pulp canal*) transmits the nerves and vessels to and from the pulp cavity through the apical foramen.

Surface of the tooth has too many slots which can be easy occupied by micro organism (41)

### 3.3.2 The Dental Pulp (*pulpa dentis*)

A rose connective tissue files a hollow of the crown (*pupla coronalis*) and the roots channel (*pulpa radicularis*). The chief function of the pulp is the formation of the dentin. Cells of the pulp are fibrinoblasts, reticular cells and plasmatic cells. The pulp contains blood vessels and nerves that enter through the apical foramen. The blood vessels of the pulp are freely branches. This brands intervening between the odontoblasts up to the layer of the predentin. Odontoblasts are very special mesenchymic cells which are obtained on the pulp. This cell has a long protoplazmatic grains in the dentin channels (Tomes grains). Nutrition substances are transported by the dentin channels which contains Tomes grains and tissue liquid. If there is no pulp it is dead tooth (42).

### 3.3.3 The Dentine (*dentin, substantia eburnea*)

The dentine creates a main part of the tooth. The color of the dentine is the light yellow. On the top of the crown is harder than on the root. It is connective tissue contains 72% of the inorganic substances mainly hydroxyapatite and 28% of the organic substances and water (42).Calcium and phosphorus are its chief inorganic components. The dentin is formed by the odontoblast and the intercellular matter. The Odontoblasts are separated between the dentin and the dental pulp, the Odontoblasts producing collagen, glykosaminoglucans and organic substances of the intercellular matter. The main essay of the odontoblasts is created dentin, to reshuffle the structure of the dentin and to participate in regeneration of the dentin (43).

### 3.3.4 The Cementum (*substantia ossea dentis)*

The cementum is the bonelike tissue that covers the roots of the teeth in a thin layer. We can recognize two types of the cementum. The first one called a acellular cementum covers approximately 2.3 of the root. Accellular cementum is closing adjacent to the dentin. The second type of the cementum is cellular cementum, covers last 1/3 of the root apex. The cellular cementum is created of the lamella. The strong sharpes grains are entered in to the cementum. The Sharpes grains are collagen fibers which anchor teeth to the bony walls of the tooth sockets in the periodontium.

### 3.3.5 The Enamel (*email*)

The enamel is the hardest tissue of the human body and it consists of 96% inorganic minerals, 0.5% organic materials and 3% water (43). Enamel's primary mineral is hydroxyapatite with the formula $Ca_5(PO_4)_3(OH)$ but is usually written $Ca_{10}(PO_4)_6(OH)_2$ to denote that the crystal unit cell comprises two molecules. Hydroxyapatite gives rigidity for tooth and bones. The different colors of the enamel maybe attributed to the variation in the thickness translucent properties, and the quality of the crystal structure and

surface stains of the enamel. The enamel is formed by the calcination hexagonal prisms (*prismata adamatina*) which are connected by the binding material (44). The enamel is formed by ameoblasts that lose their functional ability when the crown of the tooth has been completed. Therefore, enamel, after formation, has no power of further growth or repair (45).

Figure 3.6 below is for tooth anatomy,

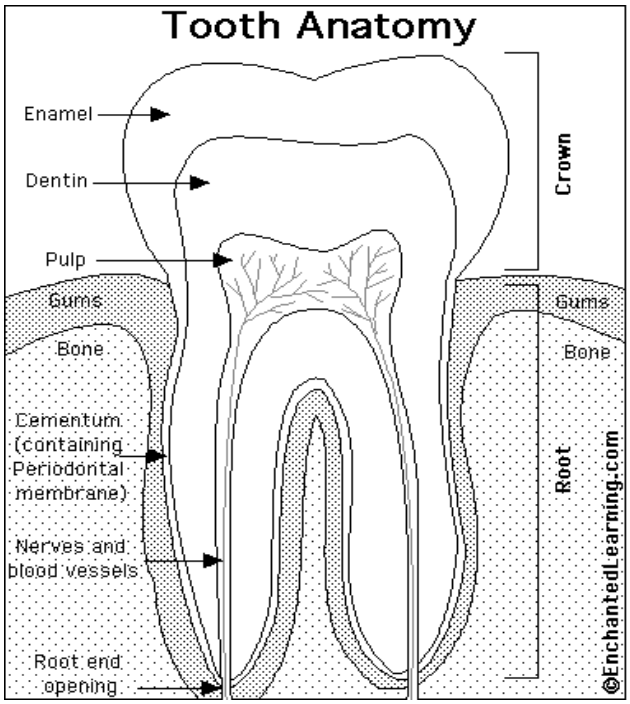


Fig. 3.6: The tooth anatomy

## 3.4 Formation and Function of Tooth Pellicle

Formation of the acquired salivary pellicle is the result of biopolymer adsorption the tooth-saliva interface. The Pellicle consists of adsorbed proteins and other macromolecules from the oral environment (saliva, crevicular fluids) and is clearly distinguished from the microbial biofilm (plaque).1 Bacterial colonisation of pelicula conduce to creation of the plaque (46).

### 3.4.1 Formation of the Pellicle

Formation of the acquired pellicle is a highly selective process since only a fraction of the proteins available in saliva is found in the pellicle.1

The first stage of pellicle formation is characterized by an almost instantaneous adsorption of salivary proteins on the enamel surface. This adsorption process starts within seconds and probably takes a couple of minutes to be completed. The thickness of this initially adsorbed layer ranges between 10 and 20 nm (46).

Initial adsorption of discrete proteins is thought to occur by electrostatic interactions with the hydrophobic regions of the tooth, leaving hydrophobic parts of the protein molecules exposed at the surface. As a second step protein aggregates or micelle like structures may adsorb to uncovered sites on the tooth surface and also interact with the initially formed hydrophobic protein layers.

#### 3.4.1.1 Composition of the Pellicle

**Proteins**

In general proteins and glycoproteins are the major salivary components of the pellicle. The pellicle formation also contains a large number of specific proteins.

Enzymes such as the salivary $\alpha$-amylase and lysozyme, as well as bacterial glucosyltransferases are immobilized in the pellicle layer.

Plasma components, such as fibrinogen, fibrinectin, albumin and IgG have been detected in the pellicle formed.

These proteins have been found on a greater extent in pellicles formed at the gingival part of the tooth surface than a t the incisal part. Significantly more plasma proteins are detected on the pellicle layer formed on the gingival part of the tooth than compared to the incisal part of the tooth.

**Carbohydrates**

The pellicle contains glucose and galactose in approximately the same concentrations. Also mannose, fucose, glucosamine and galactosamine have been detected in the pellicle layer.

**Lipids**

Lipids account for about 22-23% of the dry weight of the pellicle. The major lipid classes identified in the pellicle are

a) Neutral lipids, which are rich on free fatty acid, triglycerides, cholesterol and cholesteryl esters.
b) The phospolipidus which have a high content of phosphatidylethanolamine, sphingomyelin and phosphatidylcholine
c) The glycolipids, which consist of neutral and sulphated glyceroglucolipids.

## 3.4.2 Function of the Pellicle

### 3.4.2.1 Lubrication of the Tooth Surface

The tooth surface is lubricated by the pellicle; this is making mastication and speech more comfortable. The pellicle layer reduces friction between antagonistic teeth and between the teeth and mucosa. The pellicle layer protects the tooth surface against abrasive damage and excessive tooth wear.

#### 3.4.2.2 Semi-permeable Barrier

The pellicle acts as a barrier, which is important in maintaining the integrity of the enamel surface by preventing demineralization and by facilitating remineralisation. The pellicle have ability to modify the acid diffusion and the transport of calcium and the phosphate ions in and out from the enamel surface and this is considered to play an important moderating role in the demineralization of the enamel.

The pellicle provides a medium through which fluoride, calcium and phosphate are delivered during recalcification. At the same time it provides a certain protective function against demineralization from microbial acid and against erosive challenges. The pellicle layer reduces and retards enamel demineralization during acid exposure, but does not completely inhibit acid-related changes to the enamel surface (46).

## 3.5 Mouth Medications

### 3.5.1. Oral Cavity

The oral cavity is the beginning of the digestive tract. The bony support consists superiorly of the maxilla and inferiorly of the mobile mandible, attached by the temporomandibular joint. The oral cavity contains hard and soft tissues, saliva, the mouth micro flora, tongue.

Saliva lubricates and protects the teeth, the tongue, and the tender tissues inside the mouth. Saliva is produced in and secreted from the major paired parotid, submandibular and sublingual glands as well as from the minor glands of the oral mucosa. Human saliva is mostly composed of water (99.5%) but also includes antibacterial compounds, electrolytes, mucus and various enzymes. The mean pH of saliva is between 6.75 and 7.25.

Organs and tissues are influenced by changing properties of the external surrounding mainly by food intake (42).The temperature inside the oral cavity is between 35-36°C. This temperature provides stabile conditions for growing up large spectra of the micro organisms first of all *Streptococcus mitis, Streptococcus salivarius* (more then 70%), *Streptococcus sanguis*, *Actinomyces naeslundii* and the bacteria of the genus Rothia, Nocardia, *Bacterionema, Leptotricha, Veillonella*. The temperature is important for metabolism and enzymatic activity of the bacteria, but also for keeping the normal quality of the mouth (51).

### 3.5.2 Chlorhexidin

In this study was a used medicament containing chlorhexidine digluconat. Chlorhexidine, it is the most effective and most thoroughly tested antiplaque and antigingivitis agent known today.

Chlorhexidin *(shortened CHX)* is a cationic biguadine with very low water solubility (50). CHX is perhaps the most widely used antimicrobial agent in antiseptic products. CHX is an antimicrobial substance, which is effectual on the Gram-positive (*Staphylococcus aureus*, *Streptococcus mutans*) and with less action on the Gram-negative bacteria (*Escherichia coli*, *Proteus*,

*Bacillus*, *Pseudomonas aeruginosa*), yeasts, dermatophytes mildew and fungi *(Candida albicans*).CHX is strongly adsorbs to bacterial membranes, causing leakage of small molecules and precipitation of cytoplasmic proteins. It is active at pH 5.5-7.0 (50). CHX reduced the number of bacteria in the saliva by 30-50% and in plaque by 55-97% without producing bacterial resistance or appreciable shifts in the composition of the micro flora.

Oral toxicity is low because it is poorly absorbed from the alimentary tract (50).

CHX solution is used for rinsing of the oral cavity twice a day for one minute. Solution is used for short treatment of gingivitis and oral mucosa. Also is used as a prevention of infection after surgery.

# 4. Materials and Methods

## 4.1 Reagents

The reagents used in this work along with the name of the suppliers are presented in table 4.1.

Table 4.1: List of the reagents with name of suppliers

| Reagent | Supplier |
|---|---|
| Ammonia 25% | Merck, Darmstadt, Germany |
| Albumin fraction | Merck, Darmstadt, Germany |
| Waterless ethanol | Merck, Darmstadt, Germany |
| Hydrogen peroxide 30% | Merck, Darmstadt, Germany |
| Nanopowder of hydroxyapatite (HAP) <200nm | Sigma-Aldrich Chemie, Steinheim,Germany |
| Potassium hydroxide | Carl RothGmBH & Co., Karlsruhe, Germany |
| Sulphuric acid 96% | Merck, Darmstadt, Germany |

The solutions used in the experiments carried out as part of this work are presented in table 4.2.

Table 4.2: List of solutions and their respective ingredients and preparation protocol

| Name | Reagents | Quantity | Method of Preparation |
|---|---|---|---|
| Solution of BSA | Albumin fraction<br><br>Distilled water | 1,0 g<br><br>10,0 ml | Albumin was dissolved in Distillation water |
| Solution of hydroxyapatite 0,5% | Nanopowder of hydroxyapatite<br><br>Waterless ethanol | 1.25 g<br><br>250 ml | Hydroxyapatite was dissolved in 250.0 ml Waterless ethanol at room temperature. |
| Solutions of potassium hydroxide 0,1 M | Potassium hydroxide<br>Millipore water | 5.61 g<br><br>1000,0 ml | Reagent was dissolved in 1000,0 ml of Millipore water |

The solutions used for surface cleaning of the gold chips are presented in table 4.3.

Table 4.3: List of the solutions for surface cleaning

| Name | Reagents | Quantity | Method of Preparation |
|---|---|---|---|
| Kape | Potassium hydroxide<br><br>Hydrogen peroxide | 70,0 ml<br><br>70,0 ml | Hydrogen peroxide was added to Potassium hydroxide |
| Piranha | Hydrogen peroxide<br><br>Sulphuric acid | 35,0 ml<br><br>105,0 ml | Hydrogen peroxide was slowly added to sulphuric acid |
| Waperam | Ammonium<br><br>Hydrogen peroxide<br><br>Distilled water | 20,0 ml<br><br>20,0 ml<br><br>100,0 ml | Reagents were mixed |

Preparing of no sterile artificially saliva used in this work is presented in table 4.4.

Table 4.4: Preparing of no sterile artificially saliva

| Component | Concentration | Per 100 ml |
|---|---|---|
| Trypticase peptone (triptone) | 0,5% | 0,5g |
| Proteose peptone | 1,0% | 1g |
| Yeast extract | 0,5% | 0,5g |
| Kalium chloride | 0,25% | 0,25g |
| Part purified pig gastric mucin | 0,25% | 0,25g |
| Hemin | 5mg/l | 0,0005g |
| Menadione | 1mg/l | 0,0001g |
| Urea | 1mmol/l | 0,006g |
| Arginine | 1mmol/l | 0,02107g |

**Preparing of Filtered Saliva (pool)**

Saliva was collected from four healthy subjects at least two hours after eating and drinking. The secretion of saliva was stimulated by chewing a wax stick. Polled saliva was filtered using a paper filter at first was used filter paper 1.2 μm Whatman FP 30/1.2 CA as a second was used sterile filter FP 30/0,45 CA-S. The filter was placed on a glass funnel and saliva was let percolate through the membrane into the flask.

## 4.2 Instruments

The different instruments which used in this work are listed in table 4.5.

Table 4.2: List of instruments used in this work

| Instrument | Manufacturer |
|---|---|
| SPR device | Plasmonic Biosensoren, AG, Wallenfels, Germany |
| SPR chip | Plasmonic Biosensoren, AG, Wallenfels, Germany |
| Analytical balance | Sartorius CP225D-OCE, Sartorius AG, Götitingen, Germany |
| Hot plate | MSH-Basic, Ika-Werke, Germany |
| Ultrasound Water Bath | Bandelin electronic, frequency 35 kHz, Germany |
| Ultrasound Water Bath | High voltage power supply MCM 35-2000, Fug Electronic, Germany |

## 4.3 Preparation of SPR Chips

### 4.3.1 Surface Cleaning and Surface Activating of the Gold Chips

Cleaning is one of the most important steps for surface activation of chips and also for successful function of SPR measurements. Each SPR prism is cleaned to remove all adhering hydrophobic and hydrophilic substance from the gold surface. The cleaning process usually does not destroy the gold coating of the surface of the glass prism. The prisms were first cleaned in Piranha solution followed by activating of the gold surface with Kape solution and Waperam solution. Surface of gold chips had hydrophobic character before cleaning.

Piranha solution was first step of cleaning. The flask was filled with 140 ml Piranha solution. Twenty gold chips in holder were immersed into Piranha solution for the period of 20 minutes. After 20 minutes, chips were washed

with running distilled water for 3 minutes. Chips were worked out from holder and were inserted into desiccators. Work with Piranha solution requires delicate handling. In the next step surface of the gold chips was activated by Kape solution and Waperam solution. Activating was initiated with using of Kape solution. The flask was filled up with 140ml Kape solution. 20 gold chips in holders were laid down into this solution inside a flask. After this operation, the whole flask was inserted into the water bath heated up on temperature between 55 to 60°C for cleaning. Cleaning process lasted 20 minutes. After this time, chips was taken out from the water bath and washed up in running distilled water to remove dirty elements. Kape was slowly washed away from the flask by the distilled water. This lasted approximately 1minute. Afterwards, chips was taken out from the holder and inserted into the desiccators at room temperature.

The second method was activating with Waperam solution. A flask was filled with 140 ml Waperam solution. Twenty gold chips were immersed into Waperam. The flask was loaded into a water bath (70°C) for 10 minutes. After that, the chips was pulled out of the water bath and washed with running distillated water for approximately 1 minute. Finally, these chips were pulled out from the holder and inserted into desiccators for next operation.

### 4.3.2 Coating with Hydroxyapatite

After functionality of the gold surface of the SPR chip, hydroxyapatite was spread on the activated surface with using of the following method. Suspension of the HAP nanopowder was prepared by addition of 0.5g HAP nanopowder to 250 ml waterless ethanol and subsequently ultrasonically dispersing in a 35 kHz ultrasonic bath for 30 minutes. For coating, elecrophoretic method with using of gold chips as electrodes has been established. 12ml HAP solution was used as an electrolyte. The distance in between two electrodes was approximately 5-6mm. The electrodes were placed parallel to each other in the suspension. The electrodes was dived into the suspension and supplied with 5V electric tension for 10s. Because of

fact that HAP has a positive charge in suspension, deposits of HAP have been found on the cathode.

## 4.4 SPR Measurements

### 4.4.1 Setup

The SPR based assays described in this work was developed on the Plasmonic® SPR device (Plasmonic Biosensoren AG, Wallenfels, Germany). The device works on the well-known Kretschmann attenuated total reflection (ATR) configuration (section 3.1.2.1). Each SPR chip is made of a glass prism coated uniformly with gold to a thickness of 50 nm, which acts as the reflecting and sensing surface (Fig. 4.1). The approximate dimensions of the prisms are length = 25 mm, breadth = 10mm, thickness = 3mm. The device is characterised by a cuvette-based system, providing 8 parallel channels.

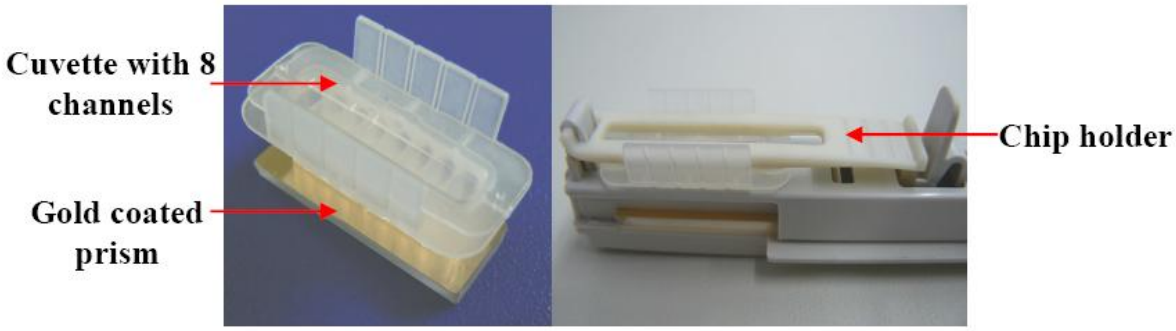


**Fig. 4.1:** Photographs showing (left) the cuvette with 8 channels placed on top of the gold-coated glass prism (right) the prism with the cuvette mounted on the chip holder

The samples and reagents are loaded into a micro-titre plate, from where the auto sampler loads them automatically into the channels of the cuvette (Fig. 4.2).

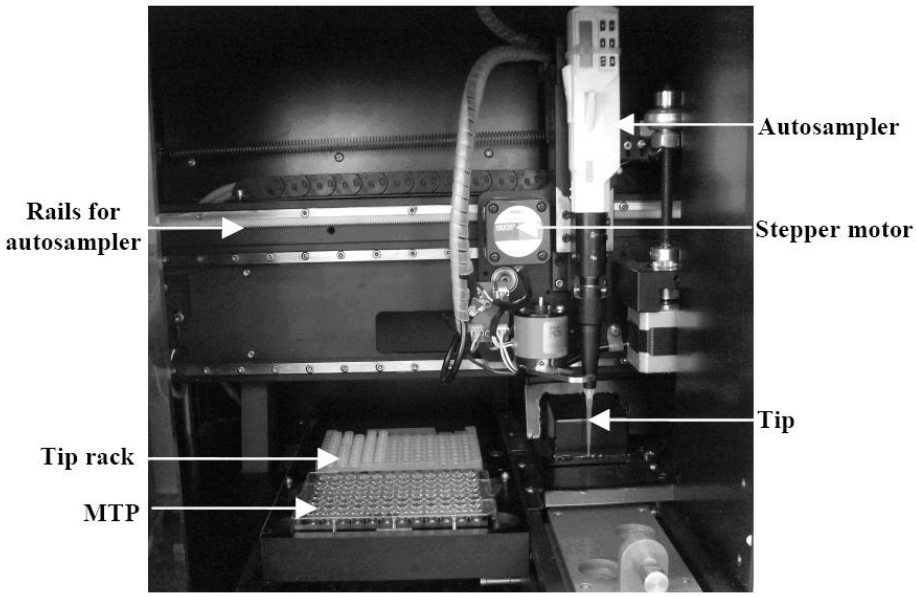


**Fig4.2:** Photograph showing the autosampler of the Plasmonic® SPR device. Movement of the autosampler is by means of a stepper motor. The autosampler moves on rails. The tips and samples are loaded on the tip rack and MTP, respectively. All operations of the autosampler are computer controlled.

The computer controls the operations of the autosampler; this control is based on a coordinate system of operation. The coordinate system of operation is described in Fig. 4.3. Another advantage of this cuvette-based system is that the sample materials can be examined without any danger of blockage, as encountered in case of fluidic-based systems. A sample volume of only 10 µL is required for analysis. The temperature is controlled by means of Peltier elements.

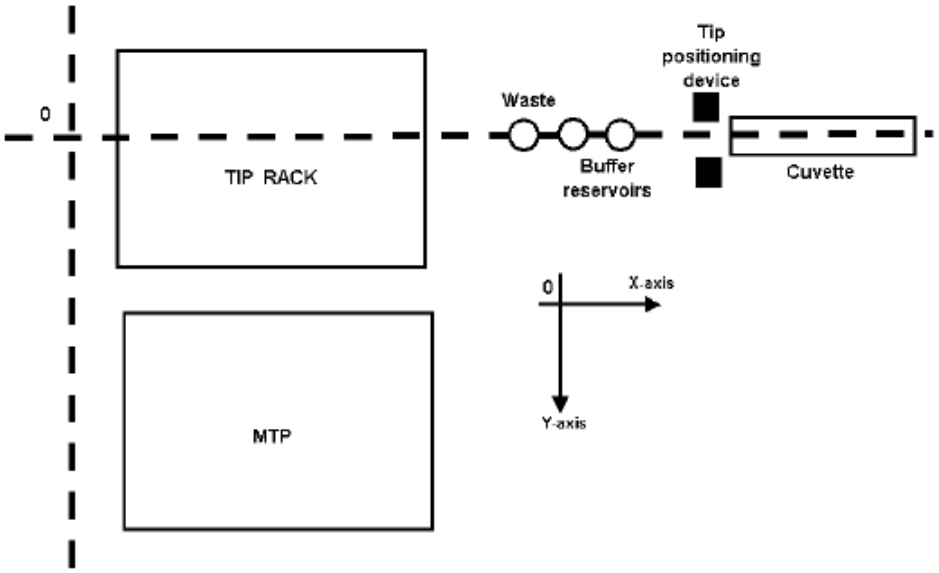


**Fig. 4.3:** The coordinate system of operation of the autosampler. The origin "O" of the coordinate system corresponds to the initialisation point of the autosampler, which is attained during the instrument start up (defined by reference switches). Operation in the Y-direction is realized by moving the MTP and TIP tray (controlled by a stepper motor). The pipette of the autosampler moves along the X-Z plane (controlled by two stepper motors). Note that the Z-axis is perpendicular to the X-Y plane. A photoelectric barrier is used to determine accurately the X- and Z- position of the pipette tip (tip positioning device)

### 4.4.2 Optics

The unique feature of the Plasmonic® SPR device is its defocusing optics. The source of incident light is a laser diode (786 nm). It emits an elliptical beam of light, which is then converted, using the cylindrical lens system of the device, into a divergent beam. Using the defocusing optics, it is possible to cover all possible angles of incidence required for the real-time determination of the SPR angle on the gold surface. The optical setup of the device is explained in Fig. 4.4a. The reflected light is detected with the help of a charge-coupled device (CCD) camera. The CCD camera receives all the light reflected from the surface of the SPR chip. The breadth of the CCD camera receiving the reflected light consists of 752 pixels for each channel.

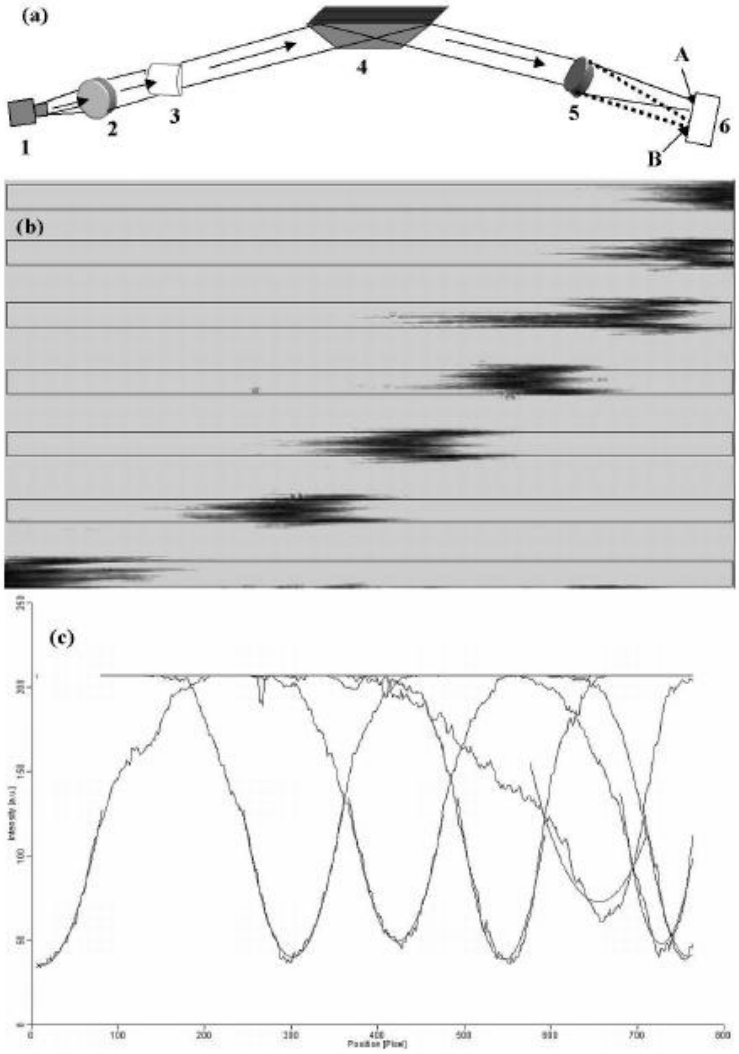


**Fig. 4.4:** The Plasmonic® SPR device. **(a)** The optical setup of the Plasmonic® SPR device: 1. Laser diode (786 nm), 2. Collimating lens, 3. Cylindrical lens resulting in a divergent beam, 4. Gold-coated SPR chip, position adjusted to obtain maximum coverage of the gold surface by the divergent beam, 5. Lens to concentrate the reflected beam of light on, 6. CCD camera. Pixel position "A" of minima at the beginning of the run. Change in pixel position to "B" at the end of the run due to a binding event on the surface of the SPR chip. (b) A view of the channels of the device. Plasmons are seen as dark spots, for different concentrations of NaBr: highest refractive index (30% NaBr) on the extreme left and lowest refractive (1.25% NaBr) at the extreme right. (c) Corresponding plot of intensity (Y-axis) of reflected light vs. Position [Pixel] (X-axis) of reflected minima, as seen on the computer screen. Each curve shows different channels corresponding to different concentrations of NaBr solutions.

The change in pixel position of the reflected minima, occurring with each binding interaction on the gold surface, is monitored by the camera. The software allows for the real-time visualisation of the minima for each channel, which are shown as dark spots on the computer screen (Fig. 4.4b). The software also generates a plot of light intensity (Y-axis) vs. pixel position (X-axis) for each channel.

The pixel position of the reflected minima for the lowest refractive index of the sample solution, starts at 752 pixels and shifts towards 0 pixel with increasing refractive index (Fig. 4.4c). The software continuously monitors this change in pixel position of the minima occurring on the CCD camera for each channel with respect to their position at the beginning of the run. This change correlates with the change in SPR angle, occurring with each binding event. The plot of change in SPR angle with time is called the “sensor gram”.

### 4.4.3 Measurement with SPR Chips

The chips coated with hydroxyapatit was inserted into sensor chip holder and covered with cuvete frame. The cuvete frame obtains 8 channels with volume 40µl. The holder was inserted into SPR device. SPR was set for automatic operations.

The first step of operation was washing the chip with 15 µl of the distillate water. After removing distillate water a volume of 15 µL of the BSA was added onto the hydroxyapatite coated chip. After incubation for 15 min the cuvette was washed again with distillate water. A good binding signal, which was stable on washing with BSA, was obtained.

Measurements with native and artificial saliva were made same way as measurements with BSA.

### Measurement with Medical Solution

Measurements with the medical solution were started with 15µl of the distillate water. Distillate water was running for 3 minutes over the chip and then was removed. In the next step 15µl of the native saliva was added on to

the coated chip for 5 minutes. Subsequently 15µl of the medical solution was rinsing chip for 2 minutes. As the last step the medical solution was washed away with natural saliva.

# 5. Results and Discussion

### 5.1 Formation of an Artificial Tooth on the Gold Surface

The first and very important step was to develop an artificial tooth. A simulation of the artificial tooth was performed on a clean gold chip, which was coated with the hydroxyapatite. The hydroxyapatite is the main inorganic component of the tooth enamel.

Suspension for electrophoretic experiments were prepared by ultrasonic agitation of hydroxyapatite nanopowder in waterless ethanol. Different concentrations were used for coating (Table 5.1) of the hydroxyapatite nanoparticles, with higher concentration of the solution, it was observed that the layer on the gold chip will be thicker, and it will not be possible to use the chip for SPR measurements. For this reason, lower concentration of solution was tested. Finally the best results were achieved with 0.5% concentration of the hydroxyapatite nanoparticles.

It is important to note that stable suspension is necessary for electrophoretic deposition experiments. From above optimal conditions could be achieved for a electrophoretic method.

| | | | | | |
|---|---|---|---|---|---|
| 1% | 0.8% | 0.6% | 0.5% | 0.4% | 0.2% |

**Table 5.1:** Hydroxyapatite solution concentrations used for testing.

Electrophoretic deposition experiment was performed with various voltages. Different periods of time were used for every electric voltage value. Every series of measurment was made three times, the below tables show an overview of the tested solutions.

The best values for voltage and time were 5V and 10 seconds. In this case the coated chip will be used for SPR measurments.

Table 5.2 shows different concentration of Hydroxyapatite solution which were used.

Table 5.2 (a)

| 1% Solution of the Hydroxyapatite | | | | | | |
|---|---|---|---|---|---|---|
| **Time** | **Voltage (V)** | | | | | |
| 10 min | 400 | 200 | 100 | 50 | 10 | 5 |
| 5 min | 400 | 200 | 100 | 50 | 10 | 5 |
| 2 min | 400 | 200 | 100 | 50 | 10 | 5 |
| 10 sec | 400 | 200 | 100 | 50 | 10 | 5 |
| 5 sec | 400 | 200 | 100 | 50 | 10 | 5 |

Table 5.2 (b)

| 0.8% Solution of the Hydroxyapatite | | | | | | |
|---|---|---|---|---|---|---|
| **Time** | **Voltage (V)** | | | | | |
| 10 min | 400 | 200 | 100 | 50 | 10 | 5 |
| 5 min | 400 | 200 | 100 | 50 | 10 | 5 |
| 2 min | 400 | 200 | 100 | 50 | 10 | 5 |
| 10 sec | 400 | 200 | 100 | 50 | 10 | 5 |
| 5 sec | 400 | 200 | 100 | 50 | 10 | 5 |

Table 5.2 (c)

| 0.6% Solution of the Hydroxyapatite | | | | | | |
|---|---|---|---|---|---|---|
| **Time** | **Voltage (V)** | | | | | |
| 10 min | 400 | 200 | 100 | 50 | 10 | 5 |
| 5 min | 400 | 200 | 100 | 50 | 10 | 5 |
| 2 min | 400 | 200 | 100 | 50 | 10 | 5 |
| 10 sec | 400 | 200 | 100 | 50 | 10 | 5 |
| 5 sec | 400 | 200 | 100 | 50 | 10 | 5 |

Table 5.2 (d)

| 0.5% Solution of the Hydroxyapatite | | | | | | |
|---|---|---|---|---|---|---|
| **Time** | **Voltage (V)** | | | | | |
| 10 min | 400 | 200 | 100 | 50 | 10 | 5 |
| 5 min | 400 | 200 | 100 | 50 | 10 | 5 |
| 2 min | 400 | 200 | 100 | 50 | 10 | 5 |
| 10 sec | 400 | 200 | 100 | 50 | 10 | 5 |
| 5 sec | 400 | 200 | 100 | 50 | 10 | 5 |

Table 5.2 (e)

| 0.4% Solution of the Hydroxyapatite | | | | | | |
|---|---|---|---|---|---|---|
| **Time** | **Voltage (V)** | | | | | |
| 10 min | 400 | 200 | 100 | 50 | 10 | 5 |
| 5 min | 400 | 200 | 100 | 50 | 10 | 5 |
| 2 min | 400 | 200 | 100 | 50 | 10 | 5 |
| 10 sec | 400 | 200 | 100 | 50 | 10 | 5 |
| 5 sec | 400 | 200 | 100 | 50 | 10 | 5 |

Table 5.2 (f)

| 0.2% Solution of the Hydroxyapatite | | | | | | |
|---|---|---|---|---|---|---|
| **Time** | **Voltage (V)** | | | | | |
| 10 min | 400 | 200 | 100 | 50 | 10 | 5 |
| 5 min | 400 | 200 | 100 | 50 | 10 | 5 |
| 2 min | 400 | 200 | 100 | 50 | 10 | 5 |
| 10 sec | 400 | 200 | 100 | 50 | 10 | 5 |
| 5 sec | 400 | 200 | 100 | 50 | 10 | 5 |

The surface of the gold chip was covered with the hydroxyapatite. Electrophoretic experiments revealed that hydroxyapatite particles were positively charged and moved towards the cathode under the applied field. Deposit weight for hydroxyapatite obtained on cathod was found to increase with increase of voltage and deposition time. Chips coated with high electric voltage were unusable for SPR measurments becouse of visible layer of the hydroxyapatite (Figure 5.1). When the refractive index of the covered chip had not been changed, further steps should not be implemented until the index is corrected by finding other methods for covering.

(a) (b) (c)

**Fig. 5.1**: Dfferent levels for coating. (a) Shows coating with 400V/10sec, (b) shows coating with 200V/10sec, and (c) 10V/5sec.

For verification of coating level of the hydroxyapatite, the chips had been tested with Atomic Force Microscopy (AFM). Scanning parameters were optimized and always had been saved a few pictures of different resolutions and from different parts of the hydroxyapatite layer.

This method had shown that the layer on the gold chips was not homogeneous. As series of figures 5.2 (a), (b), & (c) which show places without hydroxyapatit. Likeliest explanation is a different size of the nanoparticles in the solution. Most common size of the nanoparticles was approximately 60-80 nm. Surface was not homogenous and therefore the results of the mesurments could be marked with mistakes of the inhomogeneous surface of the sensor.

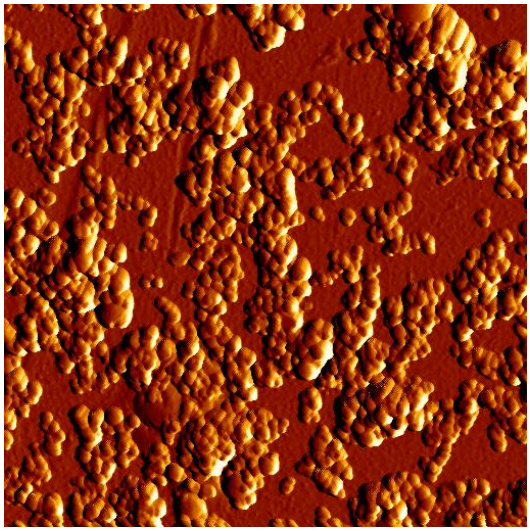

**Fig. 5.2 (a):** Surface (10 µm x10 µm) of the gold chip covered with the hydroxyapatite.Example shows hydroxyapatite layer after coating with 10V and 5 seconds.

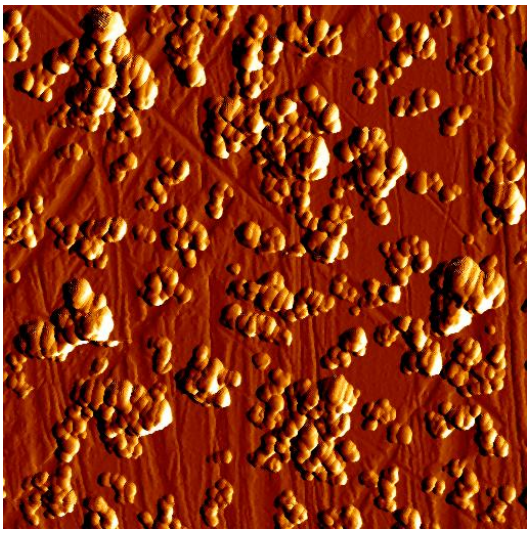

**Fig. 5.3 (b):** Surface (10 µm x10 µm) of the gold chip covered with the hydroxyapatite.Example shows hydroxyapatite layer after coating with 10V and 5 seconds.

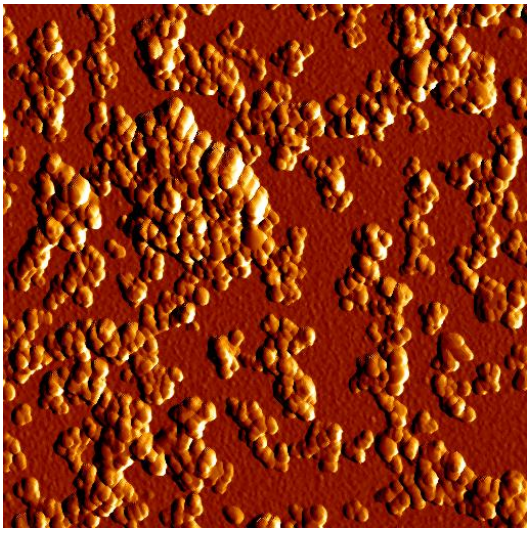

**Fig 5.3. (c):** Surface (10 μm x10 μm) of the gold chip covered with the hydroxyapatite.Example shows hydroxyapatite layer after coating with 10V and 5 seconds.

Weighing was used as a next method for checking the quantity of the hydroxyapatite on the gold chip. Every chip was marked with a number after cleaning with Kape solution and exsiccation. Afterwards electrophoretic method was used for coating. Table 5.4. shows the measured values before coating and after coating with hydroxyapatite. Approximate quantity of weighted hydroxyapatite was 58μg.

**Table 5.3 :** Weights of the chips before and after coating with hydroxyapatite

| Item | Weight Before Coating (mg) | Weight After Coating (mg) | Difference (mg) |
|---|---|---|---|
| **1** | 1705,446 | 1705,523 | 0,077 |
| **2** | 1709,331 | 1709,432 | 0,101 |
| **3** | 1693,558 | 1693,630 | 0,072 |
| **4** | 1707,567 | 1707,584 | 0,017 |
| **5** | 1688,084 | 1688,180 | 0,096 |
| **6** | 1699,539 | 1699,590 | 0,051 |
| **7** | 1720,861 | 1720,948 | 0,087 |
| **8** | 1692,151 | 1692,218 | 0,067 |
| **9** | 1689,243 | 1689,318 | 0,075 |
| **10** | 1688,741 | 1688,778 | 0,037 |
| **11** | 1707,556 | 1707,614 | 0,058 |
| **12** | 1696,052 | 1696,165 | 0,113 |
| **13** | 1707,939 | 1708,014 | 0,075 |
| **14** | 1691,724 | 1691,795 | 0,071 |
| **15** | 1698,170 | 1698,227 | 0,057 |
| **16** | 1701,534 | 1701,548 | 0,014 |
| **17** | 1676,943 | 1676,993 | 0,050 |
| **18** | 1698,684 | 1698,723 | 0,039 |
| **19** | 1697,169 | 1697,220 | 0,051 |
| **20** | 1696,873 | 1696,923 | 0,050 |
| **21** | 1710,149 | 1710,188 | 0,039 |
| **22** | 1709,202 | 1709,238 | 0,036 |
| **23** | 1694,481 | 1694,526 | 0,045 |
| **24** | 1700,269 | 1700,296 | 0,027 |
| **25** | 1642,249 | 1642,305 | 0,056 |

## 5.2 Characterisation of the Artificial Tooth

After the artificial tooth was prepared, its properties could be tested. In the first step influence of BSA bovine serum albumin protein was tested on the cleaned and activated gold chip. The sample of BSA was chosen for the reason that saliva also contains proteins and it is possible to verify if the proteins should be related to artifitial tooth.

BSA measurments were performed three times. The chip was washed by distillate water for two minutes. Subsequently, the hydroxyapatite layer was rinsed with 15μl of the BSA for 5 minutes as sensogram shows (Figure 5.4), addition of BSA led to variation of the refractive index. The following shift of the maximum could be detected: on the begginng 79nm to maximum 133nm. Subsequently, there was absorption of the protein BSA on chip. descent signal to 112nm was observed after rinsing with distillate water.

Distilled water was used for comparative measurement as blind sample. Figure 5.5 shows that distillate water does not contain any protein. Therefore distillate water will not be absorbed on the surface of the chip. For this reason refractive index, had not been changed and one straight line was observed.

Prepared sensors can be easily cleaned after use and "recycle" the removal of adsorbed proteins with Piranha solution and subsequently clean with Kape solution. Repeated use of sensor brings the total deterioration of the surface of sensor. Cleaning process could be made 3-4 times afterward could be detected non-uniform surface of the chip.

This experiment has been demonstrated that proteins, contained in the BSA, are capable of absorption on the surface of the hydroxyapatite layer. Therefore the change in signal was observed, it was confirmed that the layer on the chip is thin enough to pass the beam of the SPR and there was a change in refractive index.

The artificial tooth could be used for further testing with native and artificial saliva.

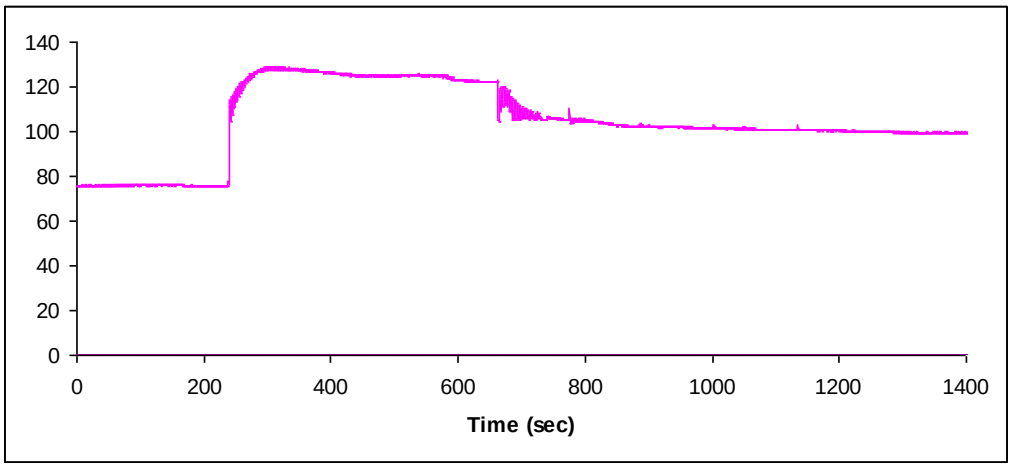


**Fig. 5.4:** Sensogram of the BSA binding on the hydroxyapatite layer. Values on the y-axis are given in nanometers.

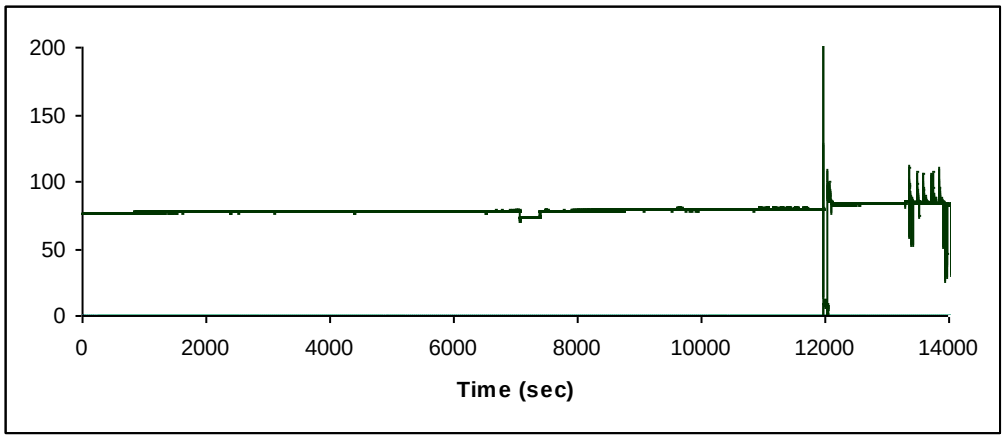


**Fig. 5.5:** Sensogram of the distillate water shows that distillate water does not contain any protein. Values on the y-axis are given in nanometers.

### 5.3 Measurements with Native and Artificial Saliva

In the first step a simulation of pellicle formation on the cleaned and covered gold chip of natural or artificial saliva was performed. The pellicle formation based on artificial saliva should be compared with formation obtained by native saliva.

The artificial tooth was washed by distillate water for two minutes. Subsequently, the hydroxyapatite layer was rinsed with 15μl of the native saliva. Measurements were made with the natural saliva and with the artificial saliva by the same procedure for three times. It was revealed that the signal of components from the native saliva resulted in a higher increase in the thickness of pellicle, whereas the artificial saliva led to a steeper rise of the binding curve. When rinsed with distilled water the thickness of the pellicle of artificial saliva decreased faster as the layer obtained by native saliva. After the rinsing process the thickness of pellicles of the different saliva were at almost the same level.

Figure 5.6 shows after the addition of native saliva was observed changing in refractive index. The value of the maximum was 520nm, and after washing with distilled water decreased the value of 478 nm. Maximum value was 392nm after addition of saliva to the surface as shown in figure 5.7. Later than washing by water, there was a rapid decline in the value of 298nm.

This difference implies that the native saliva contained a higher amount of binding proteins than the artificial saliva. It shows different behaviour of natural and artificial saliva in relation to a layer of hydroxyapatite.

Control measurements of reactions involving tests with the native saliva and the artificial saliva. Instead of the hydroxyapatite layer was used gold surface. Figure 5.8 shows native saliva binding to gold surface. Figure 5.9 shows the artificial saliva binding to gold surface.

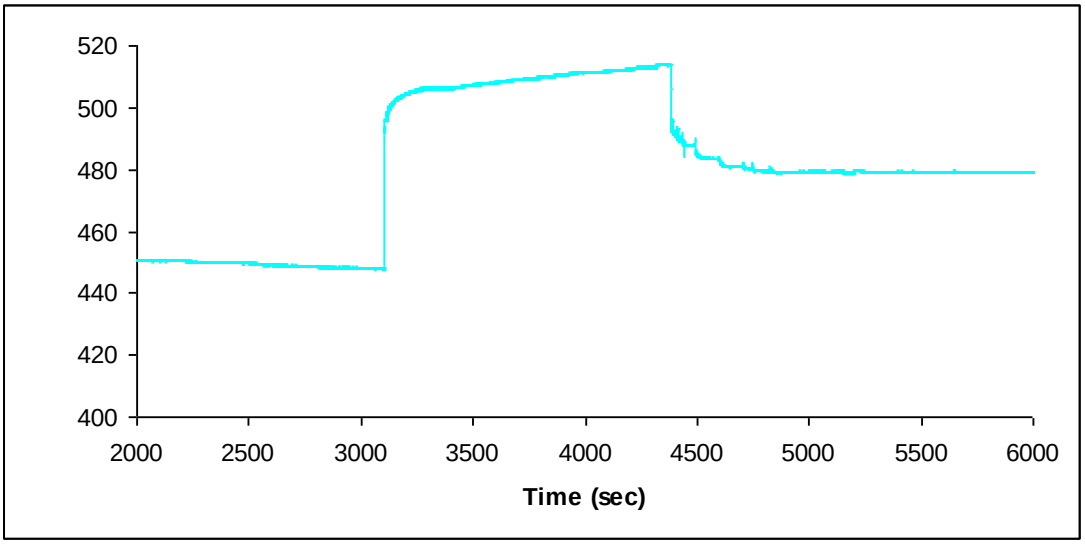


**Fig. 5.6:** Sensogram of the native saliva binding to the hydroxyapatite layer. Values on the y axis are given in nanometers.

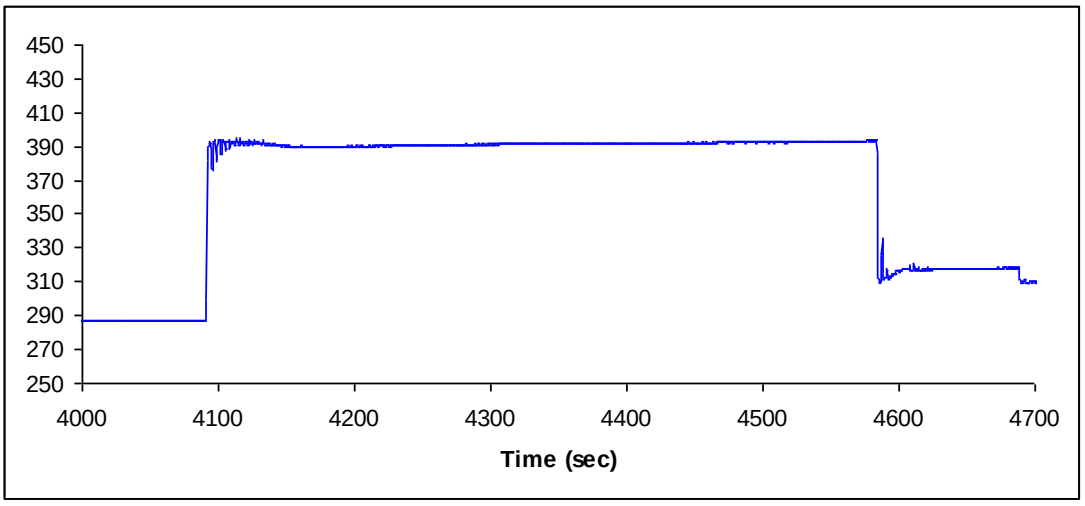


**Fig. 5.7:** Sensogram of the artificial saliva binding to the hydroxyapatite layer. Values on the y-axis are given in nanometers.

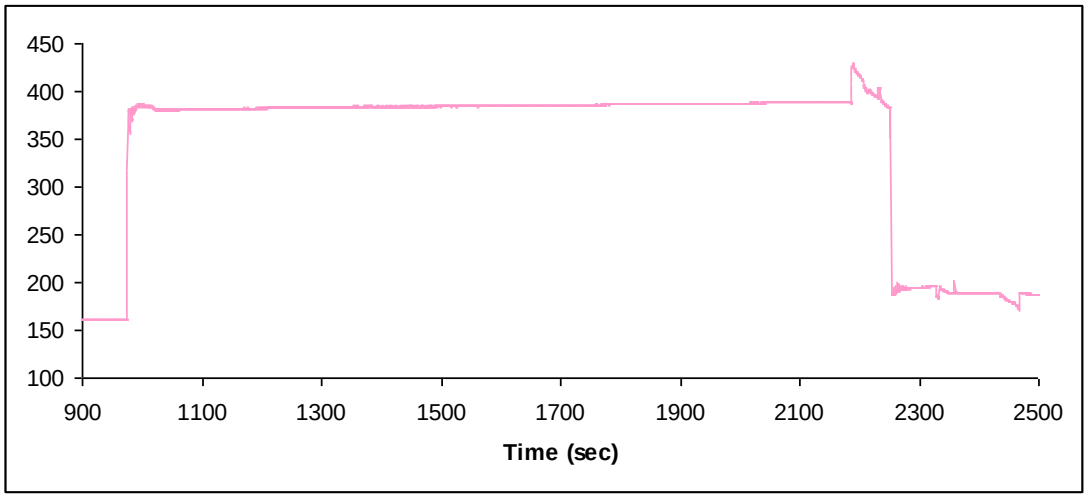


**Fig. 5.8:** Sensogram of the nativa saliva bidning on the gold surface. Values on the y-axis are given in nanometers.

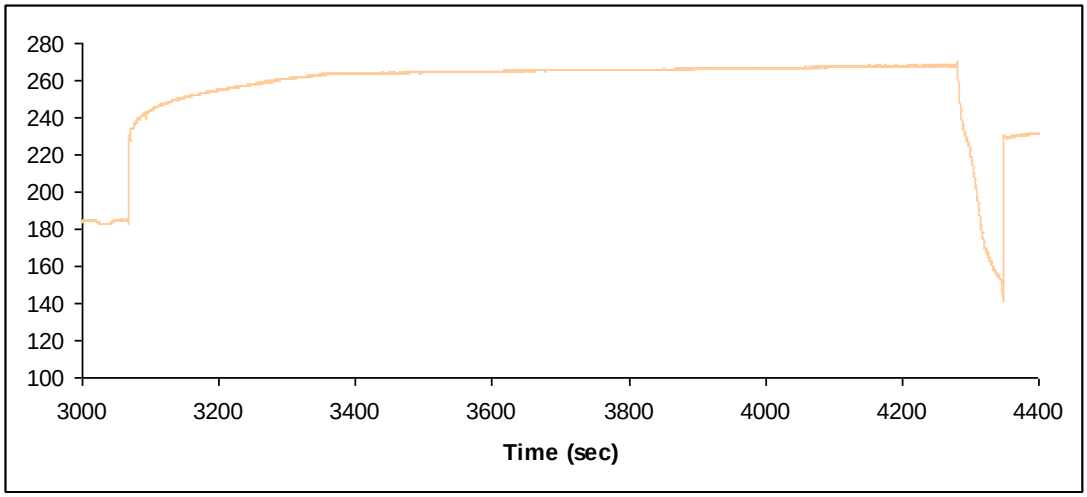


**Fig. 5.9:** Sensogram of the artificially saliva binding to the gold surface. Values on the y-axis are given in nanometers.

### 5.4 Measurements with Mouth Medications

Demonstration the adsorption of the native saliva components on a hydroxyapatite chips can be detected, an attempt was made to find out whether an exertion of influence of a pharmaceutically effective component would be detectable. Two solutions for mouth hygiene were choosed. Chlorhexamed Fluid 0.1% and Chlorhexamed 0,06% with added Fluor. Active ingredient of the preparations is the Chlorhexidine digluconat, which is being used for long period of time in dental surgery.

Through these measurements we wanted to preserve identical conditions to which are in the mouth. Experiment had been done in the temperature of 36°C.

At the beginning the coated chip was washed with 15μl of the distillate water for two minutes. Subsequently, the hydroxyapatite layer was rinsed with 15μl of the native saliva. The value of the maximum was 260 nm. After addition of the Chlorhexamed fluid 0,1% value of the maximum increased to maximum 373nm. Following rinsing was made with native saliva. Every measurments were made three times

As shown in figure 5.10, after the adding of Chlorhexamed fluid 0,1% and washing with native saliva, the increase of signal was observed. It means that the antimicrobical matter was linked on to the surface of the artificial tooth. After washing with the native saliva the increase of measuring signal was observed again. It means that saliva proteins were shifted away with using of chlorhexidin and the new layer of native saliva could be linked to the hydroxyapatit again.

Measurments with Chlorhexamed 0.06%+NaF (Figure 5.11) was made by same way as measurments with Chlorhexamed 0.1%. As first was used 15μl of the distillate water. There was detected the same behaviour on the pellicle formation, increasing to maximum value of 286nm. After adding Chlorhexamed O.O6%+NaF was observed growing signal to maximum of 386nm. Following rinsing was made with native saliva. Every measurments were made three times

Control measurements of reactions involving tests with the native saliva with chlorhexamed preparats on the gold surface, figure 5.12 shows control test with Chlorhexamed 0.1% on the gold and Figure 5.13 shows control test with Chlorhexamed 0,06%+NaF.

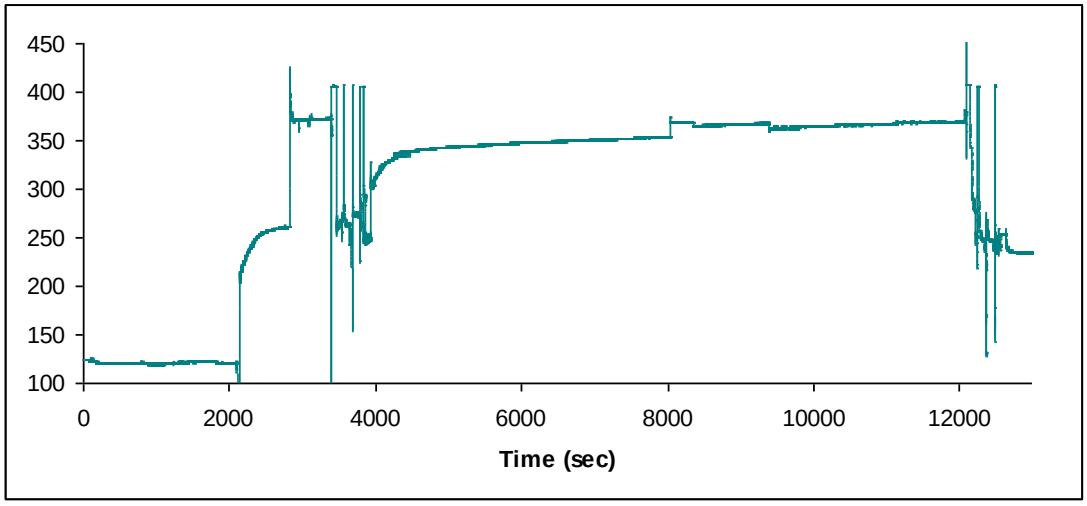


**Fig. 5.10:** Sensogram of the native saliva with CHX 0.1% on the hydroxyapatite layer. Values on the y-axis are given in nanometers.

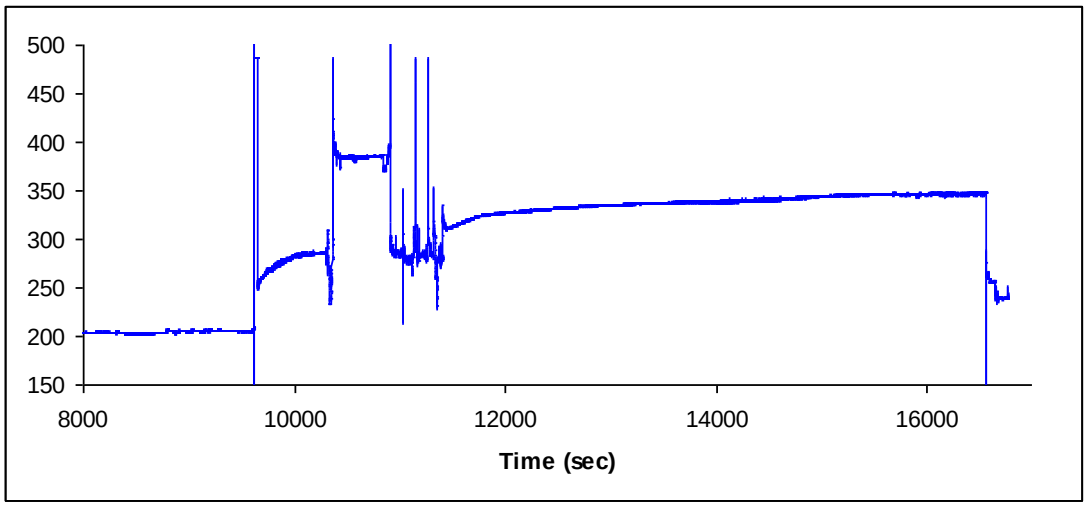


**Fig. 5.11:** Sensogram of the native saliva with CHX 0.6% + NaF to the hydroxyapatite layer. Values on the y-axis are given in nanometers.

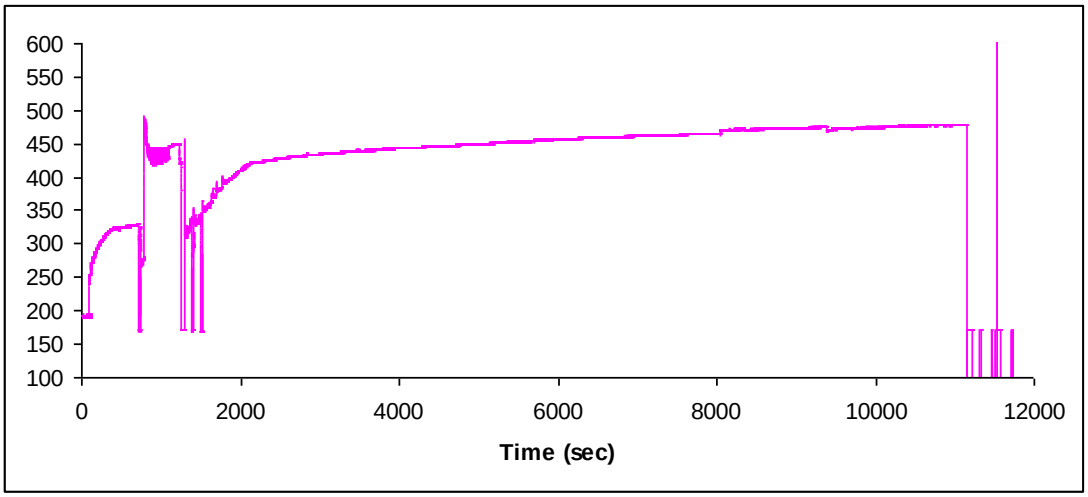


**Fig. 5.12:** Sensogram of the native saliva with CHX O.1% on the gold surface. Values on the y-axis are given in nanometers.

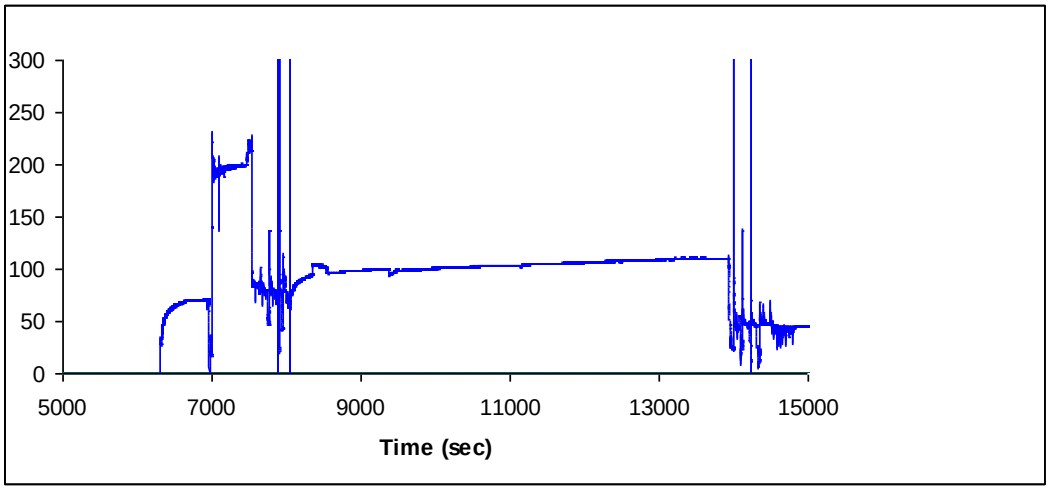


**Fig. 5.13:** Sensogram of the native savlia with CHX 0.O6% on the gold surface. Values on the y-axis are given in nanometers.

The measurement concerning the exertion of influence of a pharmaceutically effective component demonstrates that such an influence can generally be detected by SPR. Since Chlorhexamed fluid was used instead of a solution of pure chlorhexidinedigluconate, it can not be decided if the increase in

thickness is only due to this agent. The quick decrease in the thickness by rinsing with native saliva reveals that the components of the Chlorhexamed fluid can be easily removed from the surface. Some compounds of the medication, preferably chlorhexidine, bind tightly to the formed pellicle. The structure of the pellicle might be altered through the agent. It could further be shown that a treatment with Chlorhexed fluid does not result in the destruction of the bio-layer.

The presented method is very well suited to describe dynamic effects in the formation of pellicles. The effects of experimental factors such as the addition of oral therapeutically adjuvant to the dynamic of the pellicle forming process can be described with high accuracy under standardized conditions.

# 6. Conclusion

For development of an artificial tooth hydroxyapatite nanoparticles solution was electrophoretically deposited on the gold chip. It was established an experimental conditions of solution preparation, electrical field had marked effect to thickness of the hydroxyapatite layer. By this way chip suitable for SPR measurements was prepared. In the first step the bovine serum albumin (BSA) was chosen as the model protein shows absorption on the hydroxyapatite layer. Further the native saliva and artificial saliva were used for pellicle forming. Samples of saliva showed differences between binding behaviors on the hydroxyapatite layer. The application of chlorhexidingluconate pharmaceuticals on the pellicle shows increase in thickness but rinsing with native saliva disclosed that the components of chlorhexidingluconate pharmaceuticals can be easily removed from the surface.

# 7. Abstract

For development of an artificial tooth hydroxyapatite nanoparticles solution was electrophoretically deposited on the gold chip. It was established an experimental conditions of solution preparation, electrical field had marked effect to thickness of the hydroxyapatite layer. By this way chip suitable for SPR measurements was prepared. In the first step the bovine serum albumin (BSA) was chosen as the model protein shows absorption on the hydroxyapatite layer. Further the native saliva and artificial saliva were used for pellicle forming. Samples of saliva showed differences between binding behaviors on the hydroxyapatite layer. The application of chlorhexidingluconate pharmaceuticals on the pellicle shows increase in thickness but rinsing with native saliva disclosed that the components of chlorhexidingluconate pharmaceuticals can be easily removed from the surface.

# 8. References


1. Gimzewski, J.K., Reed, J., Michael A. Teitell., Malan P.G., In The Immunoassay Handbook, Wild D., Ed. Third Edition, Immunological biosensors, Elsiever, Amsterdam, 2005, pp. 265-272.

2. Ahmed, M. U., Hossain, M. M., Tamiyaa, E. 2008. Electrochemical Biosensors for Medical and Food Applications.Electroanalysis. 20 (6), 616–626.

3. Stradiotto, N.R., Yamanaka, H., Valnice, M., Zanoni, B. 2003.Electrochemical sensors: A powerful tool in analytical chemistry. J. Braz.Chem. Soc.14, 159.

4. Wang, J., Analytical Electrochemistry, VCH, New York 1994.

5. Brunetti, B., Ugo, P., Moretto, L. M., Martin, C. R. 2000. Electrochemistry of phenothiazine and methylviologen biosensor electron-transfer mediators at nanoelectrode ensembles J. Electroanal. Chem. 491, 166 174.

6. Wang, J. 2001. Glucose Biosensors: 40 Years of Advances and Challenges. Electroanalysis 13 (12), 983-988.

7. Thévenot D.R., Toth, K., Durst, R.A., Wilson, G.S., 1999. Electrochemical Biosensors: Recommended definitions and classification. Pure Appl. Chem. 71(12) 2333-2348.

8. Guilbault, G. G., Montalvo, J. G Jr., 1969. An improved urea specific enzyme electrode. Analytical Letters 2(5) 283 –293.

9. Taylor F.R, Schultz, J. S. Handbook of Chemical and Biological Sensors. Published by CRC Press, 1996.

10. Cullen, D. C., Sethi, R. S., Lowe C. R., 1990. Multi-analyte miniature conductance biosensor. Anal. Chim. Acta 231, 33.

11. Chouteaua, C., Dzyadevychc, S., Durrieua, C., Chovelonb, J. 2005. A bi-enzymatic whole cell conductometric biosensor for heavy metal ions and pesticides detection in water samples. Biosensors and Bioelectronics 21, 273–281.

12. Narayanaswamy, R, Wolfbeis, O.S. 2004. Optical Sensors, Springer, New York.

13. Moerner, W., 2007. New directions in single-molecule imaging and analysis. Proc Natl Acad Sci 104(31), 12596-12602.

14. Biran, I., Walt D. R., In Optical biosensors present and future, Part I: The present. Ligler F.S., Taitt, C.A.R., Ed. Optrode-Based Fiber Optic Biosensors (Bio-Optrode), 2002, pp. 5-56.

15. Aoyagi, S., Kudo, M., 2005. Development of fluorescence change-based, reagent-less optic immunosensor. Biosensors & Bioelectronics 20(8), 1680-1684.

16. Algar, W., Krull, U., 2008. Quantum dots as donors in fluorescence resonance energy transfer for the bioanalysis of nucleic acids, proteins, and other biological molecules. Anal Bioanal Chem 391(5), 1609-1618.

17. Cush, R.; Cronin, J. M.; Stewart, W. J.; Maule, C. H.; Molloy J.; Goddard, N.J. 1993. The resonant mirror: a novel optical biosensor for direct sensing

of biomolecular interactions Part I: Principle of operation and associated instrumentation. Biosensors & Bioelectronics 8, 347-353.

18. Kinning, T, Edwards, P., In Optical biosensors present and future, Part I: The present. Ligler F.S., Taitt, C.A.R., Ed. The Resonant Mirror Optical Biosensor, 2002, pp. 253-276.

19. Ekgasit, S., Thammacharoen, C., Knoll, W., 2004. Surface plasmon resonance spectroscopy based on evanescent field treatment. Analytical Chemistry 76(3), 561-568.

20. Keusgen, M., 2002. Biosensors: new approaches in drug discovery. Naturwissenschaften 89(10), 433- 444.

21. Tüdös, A., Lucas-van den Bos, E., Stigter, E., 2003. Rapid surface plasmon resonance-based inhibition assay of deoxynivalenol. J Agric Food Chem 51(20), 5843-5848.

22. Homola, J., In Surface plasmon resonance based sensors, Wolfbeis Ed. Electromagnetic theory of surface plasmons, 2006, pp. 3-43.

23. Dunne, L., Daly, S., Baxter, A., Haughey, S., O'Kennedy, R., 2005. Surface plasmon resonance-based immunoassay for the detection of aflatoxin B-1 using single-chain antibody fragments. Spectroscopy Letters 38(3), 229-245.

24. Scholler, N., Garvik, B., Quarles, T., Jiang, S., Urban, N., 2006. Method for generation of in vivo biotinylated recombinant antibodies by yeast mating. Journal of Immunological Methods 317(1-2), 132-143

25. Wittekindt, C., Fleckenstein, B., Wiesmuller, K.H., Eing, B.R., Kuhn, J.E., 2000. Detection of human serum antibodies against type-specifically reactive

peptides from the N-terminus of glycoprotein B of herpes simplex virus type 1 and type 2 by surface plasmon resonance. Journal of Virological Methods 87(1-2), 133-144.

26. Vaisocherova, H., Mrkvova, K., Piliarik, M., Jinoch, P., Steinbachova, M., Homola, J., 2007. Surface plasmon resonance biosensor for direct detection of antibody against Epstein-Barr virus. Biosensors & Bioelectronics 22(6), 1020-1026.

27. Forzani, E.S., Zhang, H.Q., Chen, W., Tao, N.J., 2005. Detection of heavy metal ions in drinking water using a high-resolution differential surface plasmon resonance sensor. Environmental Science &Technology 39(5), 1257-1262.

28. Win, M.N., Klein, J.S., Smolke, C.D., 2006. Codeine-binding RNA aptamers and rapid determinationof their binding constants using a direct coupling surface plasmon resonance assay. Nucleic Acids Research 34(19), 5670-5682.

29. Wang, Z.Z., Wilkop, T., Xu, D.K., Dong, Y., Ma, G.Y., Cheng, Q., 2007. Surface plasmon resonance imaging for affinity analysis of aptamer - protein interactions with PDMS microfluidic chips. Analytical and Bioanalytical Chemistry 389, 819-825.

30. Zhang, S.G., 2004. Hydrogels - Wet or let die. Nature Materials 3(1), 7-8.

31. Lofas, S., Johnsson, B., Edstrom, A., Hansson, A., Lindquist, G., Hillgren, R.M.M., Stigh, L., 1995. Methods for site controlled coupling to carboxymethyldextran surfaces in surface-plasmon resonance sensors. Biosensors & Bioelectronics 10(9-10), 813-822.

32. Knoll, W.; Liley, M.; Piscevic, D.; Spinke, J.; Tarlov, M. J. AdVBiophys. 1997, 34, 231.

33. Jung, L.S., Nelson, K.E., Stayton, P.S., Campbell, C.T., 2000. Binding and dissociation kinetics of wild-type and mutant streptavidins on mixed biotin-containing alkylthiolate monolayers. Langmuir 16(24), 9421-9432.

34. Koubova, V., Brynda, E., Karasova, L., Skvor, J., Homola, J., Dostalek, J., Tobiska, P., Rosicky, J., 2001. Detection of foodborne pathogens using surface plasmon resonance biosensors. Sensors and Actuators B-Chemical 74(1-3), 100-105.

35. Busse, S.; Scheumann, V.; Menges, B.; Mittler, S., 2002. Biosens. Bioelectron. 17, 704.

36. Zhen, G. L.; Falconnet, D.; Kuennemann, E.; Voros, J.; Spencer, N. D.; Textor, M.; Zurcher, S., 2006. AdV. Funct. Mater. 16, 243.

37. Ladd, J., Boozer, C., Yu, Q.M., Chen, S.F., Homola, J., Jiang, S., 2004. DNA-directed proteinimmobilization on mixed self-assembled monolayers via a streptavidin bridge. Langmuir 20(19), 8090-8095.

38. Rusmini, F., Zhong, Z.Y., Feijen, J., 2007. Protein immobilization strategies for protein biochips. Biomacromolecules 8(6), 1775-1789.

39. Hermanson, G. T. In: Bioconjugation techniques. Academic Press, New York, 1996, Antibody modification and conjugation, pp 456-493.

40. Lazcka, O., Del Campo, F.J., Munoz, F.X., 2007. Pathogen detection: A perspective of traditional methods and biosensors. Biosensors & Bioelectronics 22(7), 1205-1217.

41. Geddes, D.A.M., Jenkins, G.N.: Intrinsic and extrinsic factors influencing the flora of the mouth in the normal microbial flora of man, London, 1974

42. Urban, F: Stomatologie, Praha: Státní zdravotnické nakladatelství,1964

43. www.lfp.cuni.cz/**histologie**/education/**doc**/teeth.pdf

44. Dokládal, M.: *Anatomie zubu a chrupu*. Brno: Masarykova univerzita – lékařská fakulta, 1994.

45. http://www.tpub.com/content/medical/14274/css/14274_58.htm

46. Basel, K. , 2006,The teeth and their Environment, vol 19, 29-64

47. Gibbons, RJ.1985: Bacterial adhesion to oral tissue: A model for infection diseases. J Dent Res. 63, 378-85

48. Collins L.M.C, Dawes C.: The surface area of the adult human mouth and thickness of the salivary film covering the teeth and oral mucosa. J Dent Res. 66. 1300-1302, 1987

49. J.I. Ingle, L.K.Bakland,J.C. Baumgartner: Ingle's Endodontics, PMPH-USA, 2008

50. Bertram G. Katzung: Basic & clinical pharmacology, McGraw-Hill Professional, 2007

51. Lynch, J.M., Poole, N.J.:Microbial Ecology,Oxford 1979.